การสังเคราะห์พอลิเอสเทอร์ที่มีพาราแอลคอกซีซินนาเมต

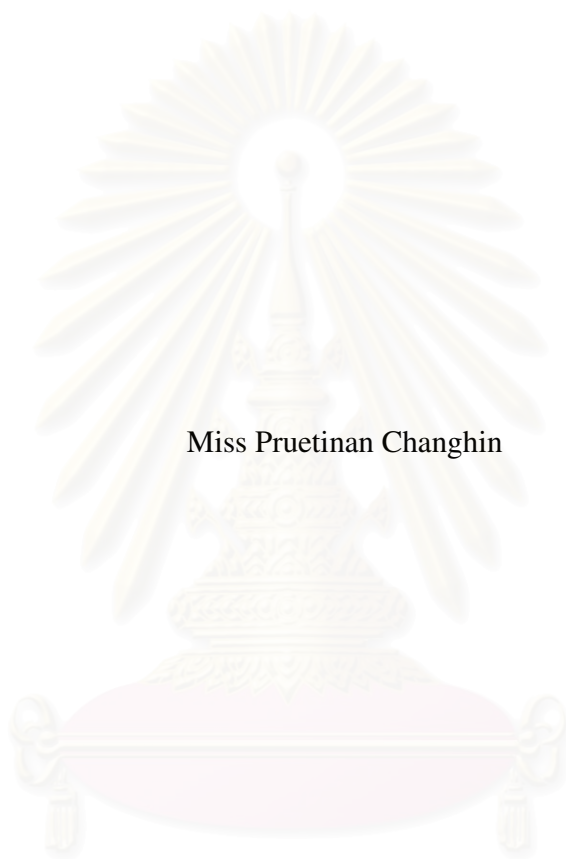นางสาวพฤฒินันท์ ช่างหิน

วิทยานิพนธ์นี้เป็นส่วนหนึ่งของการศึกษาตามหลักสูตรปริญญาวิทยาศาสตรมหาบัณฑิต
สาขาวิชาปิโตรเคมีและวิทยาศาสตร์พอลิเมอร์
คณะวิทยาศาสตร์ จุฬาลงกรณ์มหาวิทยาลัย
ปีการศึกษา 2549

SYNTHESIS OF POLYESTER CONTAINING *p*-ALKOXYCINNAMATE

Miss Pruetinan Changhin

A Thesis Submitted in Partial Fulfillment of the Requirements
for the Degree of Master of Science Program in Petrochemistry and Polymer Science
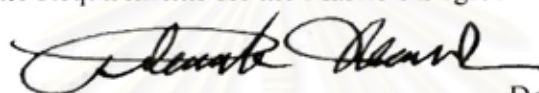Faculty of Science
Chulalongkorn University
Academic Year 2006

Thesis Title	SYNTHESIS OF POLYESTER CONTAINING p-ALKOXYCINNAMATE
By	Miss Pruetinan Changhin
Field of Study	Petrochemistry and Polymer Science
Thesis Advisor	Assistant Professor Yongsak Sritana-anant, Ph.D.
Thesis Co-advisor	Associate Professor Supason Wanichwecharungruang, Ph.D.

Accepted by the Faculty of Science, Chulalongkorn University in Partial Fulfillment of the Requirements for the Master's Degree

………………………………………….Dean of the Faculty of Science
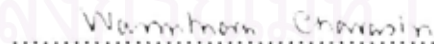
(Professor Piamsak Menasveta, Ph.D.)

THESIS COMMITTEE

……………………………………Chairman

(Associate Professor Supawan Tantayanon, Ph.D.)

……………………………………Thesis Advisor

(Assistant Professor Yongsak Sritana-anant, Ph.D.)

……………………………………Thesis Co-advisor

(Associate Professor Supason Wanichwecharungruang, Ph.D.)

……………………………………Member

(Assistant Professor Warinthorn Chavasiri, Ph.D.)

……………………………………Member

(Assistant Professor Varawut Tangpasuthadol, Ph.D.)

พฤฒินันท์ ช่างหิน : การสังเคราะห์พอลิเอสเทอร์ที่มีพาราแอลคอกซีซินนาเมต
(SYNTHESIS OF POLYESTER CONTAINING *p*-ALKOXYCINNAMATE)
อ.ที่ปรึกษา : ผศ.ดร. ยงศักดิ์ ศรีธนาอนันต์, อ.ที่ปรึกษาร่วม : รศ.ดร. ศุภศร วนิชเวชารุ่งเรือง, 70
หน้า.

งานวิจัยนี้เป็นการสังเคราะห์พอลิเมอร์สามชนิดที่มีสมบัติในการกรองรังสียูวี   โดยเริ่มจากการ
สังเคราะห์มอนอเมอร์สองชนิดคือ   1,2-(บิส(4-(2-คาร์บอกซีไวนิล)ฟีนอกซี))อีเทน (M2) และ 1,12-
(บิส(4-(2-คาร์บอกซีไวนิล)ฟีนอกซี))โดเดกเคน   (M12)   จากนั้นให้มอนอเมอร์ทั้งสองทำปฏิกิริยา
ควบแน่นกับพอลิเอทิลีนไกลคอล (PEG) ที่มีน้ำหนักโมเลกุลเฉลี่ย 200 และ 400 ได้เป็น พอลิ((1,2-(บิส
(4-(2-คาร์บอกซีไวนิล)ฟีนอกซี))อีเทน-โค-(พอลิ(เอทิลีน   ไกลคอล)200)),   พอลิ((1,2-(บิส(4-(2-คาร์
บอกซีไวนิล)ฟีนอกซี))อีเทน-โค-(พอลิ(เอทิลีน   ไกลคอล)400)) และ พอลิ((1,12-(บิส(4-(2-คาร์บอกซี
ไวนิล)ฟีนอกซี))โดเดกเคน-โค-(พอลิ(เอทิลีน   ไกลคอล)400)) พบว่าพอลิเมอร์ที่สังเคราะห์ได้มีน้ำหนัก
โมเลกุลเฉลี่ยอยู่ในช่วง 2100-2600 ดาลตัน   พอลิเมอร์ทั้งหมดสามารถดูดกลืนรังสียูวีบีได้ โดยพบว่า
โคพอลิเมอร์ M2-PEG ที่มีน้ำหนักโมเลกุลเฉลี่ย 400 มีลักษณะเป็นของเหลวสีเหลือง ละลายในตัวทำ
ละลายอินทรีย์ได้ดี   นอกจากนี้ พอลิ((1,2-(บิส(4-(2-คาร์บอกซีไวนิล)ฟีนอกซี))อีเทน-โค-(พอลิ(เอ
ทิลีน ไกลคอล)400)) และ พอลิ((1,12-(บิส(4-(2-คาร์บอกซีไวนิล)ฟีนอกซี))โดเดกเคน-โค-(พอลิ(เอ
ทิลีน ไกลคอล)400)) สามารถเตรียมให้เกิดเป็นอนุภาคนาโน/ไมโครขนาดเฉลี่ย 500 นาโนเมตร และ 3
ไมโครเมตรตามลำดับ ด้วยวิธีการแทนที่ตัวทำละลาย

สาขาวิชา..........ปิโตรเคมีและวิทยาศาสตร์พอลิเมอร์.......... ลายมือชื่อนิสิต.....................................
ปีการศึกษา...................2549........................... ลายมือชื่ออาจารย์ที่ปรึกษา.........................
                                              ลายมือชื่ออาจารย์ที่ปรึกษาร่วม.........................

v

4772393223: MAJOR PETROCHEMISTRY AND POLYMER SCIENCE

KEY WORD: ALKOXYCINNAMATE / POLYESTER / SUNSCREEN

PRUETINAN CHANGHIN: SYNTHESIS OF POLYESTER CONTAINING
p-ALKOXYCINNAMATE. THESIS ADVISOR : ASST.PROF. YONGSAK
SRITANA-ANANT, Ph.D., THESIS CO-ADVISOR : ASSOC.PROF.
SUPASON WANICHWECHARUNGRUANG, Ph.D., 70 pp.

a

This work involved the synthesis of three polymers containing UV absorptive chromophore. The first two monomers; 1,2-(bis(4-(2-carboxyvinyl)phenoxy))ethane (M2) and 1,12-(bis(4-(2-carboxyvinyl)phenoxy))dodecane (M12) were synthesized. Condensation polymerization between M2 or M12 and poly(ethylene glycol)200 (PEG200) or poly(ethylene glycol)400 (PEG400) yielded poly((1,2-(bis(4-(2-carboxy vinyl)phenoxy))ethane-*co*-(poly(ethylene glycol)200)), poly((1,2-(bis(4-(2-carboxyvinyl) phenoxy))ethane-*co*-(poly(ethylene glycol)400)) and poly((1,12-(bis(4-(2-carboxyvinyl) phenoxy))dodecane)-*co*-(poly(ethylene glycol)400)). The averaged molecular weights of all three polymers were in the range of 2100-2600 Da. Absorption profiles of all synthesized polymers indicated UVB absorption property. The M2-PEG400 copolymer, a yellowish liquid, showed good solubility in various organic solvents. In addition, poly((1,2-(bis(4-(2-carboxyvinyl)phenoxy))ethane-*co*-(poly(ethylene glycol)400)) and poly((1,12-(bis(4-(2-carboxyvinyl)phenoxy))dodecane)-*co*-(poly(ethylene glycol)400)) could be prepared as nano/microparticles with an average size of 500 nm and 3 μm respectively, through solvent displacement technique.

สถาบันวิทยบริการ

จุฬาลงกรณ์มหาวิทยาลัย

Field of study... Petrochemistry and Polymer Science ... Student's signature...พฤติษัณฑ์ ...
Academic year............................2006............................ Advisor's signature....................
Co-advisor's signature....................

ACKNOWLEDGEMENTS

CONTENTS

LIST OF FIGURES

LIST OF TABLES

LIST OF ABBREVIATIONS

br	broad (NMR)	$\overline{M}n$	number average molecular
°C	degree celsius		weight
cm^{-1}	unit of wavenumber (IR)	m.p.	melting point
cm^{-1}	per centimeter	MW	molecular weight
Cpd	compound	m/z	mass per charge
$CDCl_3$	deuterated chloroform	MS	mass spectrometry
d	doublet (NMR)	nm	nanometer
DMF	dimethylformamide	NMR	nuclear magnetic resonance
DMSO	dimethylsulfoxide	PEG	poly(ethylene glycol)
ESI-MS	electrospray ionization	ppm	parts per million
	mass spectrometry	R_f	retardation factor
g	gram	s	singlet (NMR)
GPC	gel permeation chromatography	t	triplet (NMR)
Hz	hertz	δ	chemical shift
IR	infrared	%	percent
J	coupling constant	λ	wavelength
mL	milliliter	ε	molar absorptivity
mmole	millimolar	μm	micrometer

CHAPTER I
INTRODUCTION

1.1 Effect of Ultraviolet Radiation on the Skin

Ultraviolet radiation that reaches the Earth's surface can be divided into two wavebands, UVB (290-320 nm) and UVA (320-400 nm) both of which contribute to biological changes. The adverse effects of UV radiation on normal human skin comprise sunburn inflammation (erythema), tanning and immunosuppression. Chronic effect of long-term exposure to UV radiation leads to photoaging, immunosuppression and photocarcinogenesis. Photocarcinogenesis involves the accumulation of genetic changes, as well as immune system modulation and ultimately leads to skin cancer.

UVB radiation induces sunburn [1], immunosuppression [2] and can directly interacts with DNA bases and causes DNA lesions, particularly cyclobutane pyrimidine dimers (CPDs) and pyrimidine (6-4) pyrimidone photoproducts (6-4PPs). Defective repair of these lesions leads to mutations and can cause the development of skin cancer [3,4].

UVA radiation can penetrate deeper into the dermal matrix of skin tissues than UVB does. UVA is the main cause of photoaging [5], immunosuppression [2] and DNA damage [3]. Skin damages by UVA are mediated partly by reactive oxygen species (ROS) such as singlet oxygen, superoxide anion, hydrogen peroxide and others which all are induced by UVA. UVA can also produce structural damage to the DNA (8-oxoguanine is the most common lesion), inhibits DNA repair and impairs the immune system. Recently, it has been reported that UVA produces not only 8-oxo-7,8-dihydroguanine but also induces CPDs. In 2004, S. Courdavault et al [6] showed that in human skin cells, the yield of UVA-induces CPDs was higher than that 8-oxo-7,8-dihydroguanine, the most frequent UVA-induces oxidative DNA lesions. Interestingly, in 2005, S. Courdavault et al [7] demonstrated that UVA radiation also generated cyclobutane pyrimidine dimers, which are slightly less efficiently repaired than CPDs produced upon UVB radiation.

1.2 The Development of Ultraviolet Absorber

For many years, topical sunscreens have been recommended as a useful way to provide protection to human skin against acute and chronic adverse effect of UV radiation. Sunscreens are generally classified as either chemical or physical sunscreen. The first commercial chemical sunscreen was introduced in 1928, it contained benzyl salicylate and benzyl cinnamate and in 1942, *p*-aminobenzoic acid (PABA) ointment was showed to be an effective sunburn protectant [8]. This advance led to the development of many new sunscreen agents. **Table 1.1** showed US Food and Drugs Administration (US-FDA) monograph include fourteen chemical sunscreens and two physical sunscreen agent and the maximum allowed concentration for each.

Table 1.1 US-FDA sunscreen final monograph ingredients [8]

Compound	% Maximum concentration permitted	Absorbance range (nm)
PABA (UVB)		
p-Aminobenzoic acid (PABA)	15.0	260-313
2-Ethylhexyl-o-dimethylaminobenzoate (Padimate-O), octyldimethyl PABA	8.0	290-315
Salicylates (UVB)		
2-Ethylhexyl salicylate (octyl salicylate)	5.0	250-320
Triethanolamine salicylate (trolamine salicylate)	5.0-12.0	260-320
3,3,5-Trimethylcyclohexyl salicylate (homosalate)	4.0-15.0	290-315
Cinnamates (UVB)		
2-Ethoxyethyl-*p*-methoxycinnamate (Cinnoxate)	3.0	270-328
Ethylhexyl-*p*-methoxycinnamate (Parsol® MCX, OMC, EHMC), Neo Heliopan AV	2.0-7.5	290-320
Benzophenones (UVA)		
2-Hydroxy-4-methoxybenzophenone (oxybenzone, benzophenone-3)	2.0-6.0	270-350

Compound	% Maximum concentration permitted	Absorbance range (nm)
2-Hydroxy-4-methoxybenzophenone-5-sulphonic acid (sulisobenzone, benzophenone-4)	5.0-10.0	270-360
2,2-Dihydroxy-4-methoxybenzophenone (dioxybenzone, benzophenone-8)	3.0	260-380
Dibenzoylmethane (UVA) Butyl methoxy dibenzoylmethane (avobenzone, BMDBM)	3.0	355
Miscellaneous 2-Ethylhexyl-2-cyano-3,3-diphenylacrylate (octocrylene)	7.0-10.0	290-360
Menthylanthranilate	03.5-5.0	290-370
2-Phehylbenzimidazole-S-sulphonic acid	1.0-4.0	290-320
Physical Sunscreens Titanium dioxide	2.0-25.0	250-380
Zinc oxide	25	250-380

Today, the most popular UVB filters are cinnamates, particularly 2-ethylhexyl-*p*-methoxycinnamate (EHMC), a compound with high molar absorption coefficient (22000-24000 $M^{-1}cm^{-1}$ at 309 nm), and uncommonly photoallergic sensitization proper [9,10]. Nevertheless, EHMC could penetrate into human skin [15,18,19]. The most popular UVA filters are benzophenones and dibenzoylmethane. However, benzophenones are broad-spectrum filters with solvent-dependent absorption bands and high transdermal absorption [16,18,19]. Dibenzoylmethanes have a disadvantage of photoinstability, with UVA exposure the irreversible reactions occur causing the decrease in UV absorption property.

Physical sunscreens such as titanium dioxide and zinc oxide have recently been used extensively in cosmetic sunscreens. Nevertheless, the compound tends to be opaque and white on the skin and consequently is unacceptable for cosmetic use. Over the last

decade, cosmetic industry technology has been applied to the development of microfine of titanium dioxide and zinc oxide [11,12] which particles size around 20-50 nm. They are nearly imperceptible. However recently, it has been reported that microfine titanium dioxide and microfine zinc oxide could penetrate porcine stratum corneum and human skin [13,14].

Combinations of organic and inorganic sunscreens have recently been introduced by J.R.V-Hernandez and C.C.M-Coymann [15]. The study showed that fixation of organic molecules onto the surface of the titanium dioxide crystals helped increasing UV absorption capacity in the combination of titanium dioxide crystals and the organic UV filter.

1.3 Mechanism of Chemical Absorber

In general chemical absorbers usually contain an aromatic ring conjugated with a carbonyl group. Often an electron-releasing group such as amine or methoxy group, is substituted in the ortho- or para- position of the aromatic ring. In other words, these molecules contain conjugated systems those allow electron delocalization upon absorption of photons. They absorb the harmful (high-energy) UV rays (250-400 nm) and convert the absorbed energy into innocuous longer wave (lower-energy) radiation (usually above 400 nm). **Figure 1.1** shows the mechanism of UV-absorbers.

Absorbs High Energy UV Rays (250-350 nm)

Molecule in Excited State

Emits Low Energy Rays (Longer λ)
1. Very Low E (over 800 nm)
   IR Region (Heat)
2. Intermediate E (450-800 nm)
   Visible Region (Fluorescence)
3. Low UV Region (380-450 nm)

Molecule in Ground State

Molecule Returns to Ground State
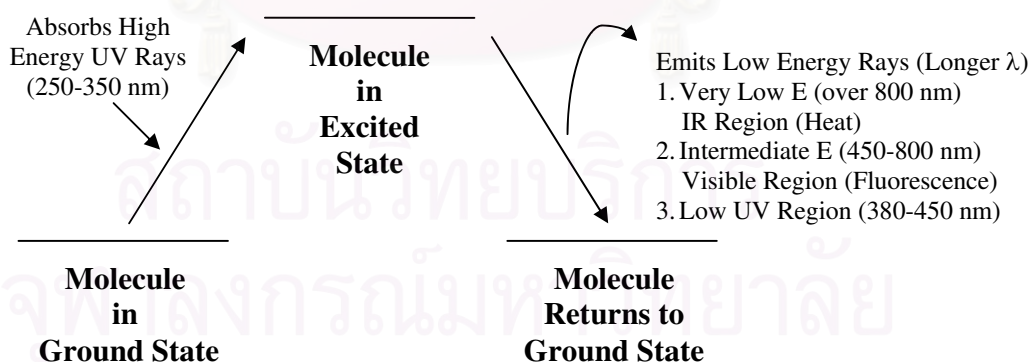
Figure 1.1 Schematic representation of the process in which a sunscreen chemical absorbs the harmful high-energy rays and renders them relatively harmless low-energy rays

1.4 Absorption of Sunscreen

Sunscreens play a significant role in our lives, they protect us against UV radiation, thus prevent sunburn, photoaging and skin cancer and minimize various photo-sensitivities. OMC is the popular UV-B screening compound used in various cosmetic formulations because it has large molar absorption coefficient (ε) and shows only few allergic reactions to human skin [9,10]. Nevertheless, transdermal permeation of the compound into human body has been reported.

In 1995, J. Hanny and R. Nagel [16] detected benzophenone-3 and OMC in human breast milk and in the same year, U.H. Leweke and B.C. Lippold [17] also detected transdermal penetrations through human skin layer of various sunscreens (octyl dimethyl *p*-amino benzoic acid, 4-isopropyl-dibenzoylmethane, 3-(4-Methylbenzylidene) -camphor, isoamyl-*p*-methoxycinnamate and oxybenzene.

In 1997, C.G. Hayden and coworkers [18] found that systemic benzophenone-3 absorption over a 10 hour period represented between 1 and 2% of the applied dose. The study could not detect OMC in urine of volunteers whose commercially available SPF 15+ sunscreen product had been applied to their forearms. This study indicated the hydrophobic nature of OMC and agreed with the fact that OMC was found in breast milk.

In 1999, V.K. Gupta and coworkers [19] studied absorption of sunscreen through Micro-Yucatan Pig Skin *in vitro* by diffusion cell technique. They observed that OMC and benzophenone-3 reached the stratum corneum within an hour host application and the amounts penetrated into viable skin and receptor fluid increased slowly over time. The study also indicated that benzophenone-3 penetrated skin to a greater extent than OMC.

G. Potard and coworkers [20] studied penetration of UV filters in various fresh human skin layers by stripping technique using HPLC for the quantification. The result obtained after exposure time of 16 hours indicated that OMC, benzophenone-3, benzophenone-4, octocrylene and octyltriazone could penetrate into stratum corneum, epidermis and dermis. However, only benzophenone-3 was found in receptor fluid.

Transdermal penetration of OMC through human skin was also demonstrated in other studies including works done by G. Potard group [21] and V.Saveiga group [22].

1.5 Solutions for Skin Penetration Problem of Ultraviolet Absorber

As mentioned earlier that penetration of UV filters is normal for several compounds. Several attempts have been made to quantify the amount of UV-absorbing chemicals which enter the body via skin. The developments of new ingredients and new delivery systems have been developed to increase the skin accumulation of UV absorbers.

In 1996, T. Carpenter and coworkers [23] included 25% adipic acid/diethylene glycol/glycerin (ADG) cross-polymer in sunscreen solutions and found out that this resulted in reduction of penetration into the viable skin of OMC and bezophenone-3, based on skin stripping experiments with human subjects.

In 2001, P. Hossel and coworkers [24] demonstrated another methodology in reducing sunscreen transdermal absorption. The technique was to use less UV filter in the formulation but with an addition of SPF enhancer. SPF enhancer could increase the skin's protection ability with less amount of UV absorber used. The author prepared N-vinylimidazole/diallylamine copolymer and used as SPF enhancer in the formulations.

In 2002, D.A. Godwin and coworkers [25] determined the influence of Transcutol® CG (diethylene glycol monoethyl ether) which was added in sunscreen formulation, on the transdermal permeation and skin accumulation of sunscreen OMC. The results indicate that inclusion of Transcutol® CG in sunscreen formulations increases the skin accumulation of the UV absorbers without a concomitant increase in transdermal permeation.

Transcutal® CG
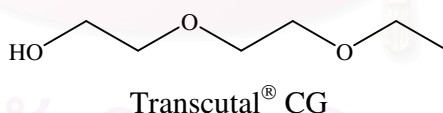
In 2003, G. Yener and coworkers [26] prepared solid lipid microspheres (SLM) which carriers for OMC in order to decrease release and penetration in SLM formulation and also enhanced the photostability of OMC.

In 2004, M.M. Jimenez and coworkers [27] investigated the influence of the carrier nanocapsule (NC) on *in vit*ro percutaneous absorption of OMC. Similar o/w and w/o emulsions of free-OMC and OMC encapsulated in NC (OMC-NC) were compared. The results showed clearly that incorporation of OMC into NC decreased the penetration of OMC.

S. Pattanaargson and coworkers [28] prepared poly[(propyl-*p*-methoxycinnamate octyl methyl)]silixane copolymer (CMOMS) through consecutive hydrosilylations using 2-propenyl-*p*-methoxycinnamate and octane. The octyl groups were introduced into the polymer to create hydrophobic environment around the chromophore and prevent possible photodimerizations between two cinnamate moieties. The result showed that the maximum absorption wavelength of the product was similar to that of OMC. Photostability test indicated that the grafted product was more stable than free OMC. Skin permeation of such polymer was much lower than free OMC.

CMOMS
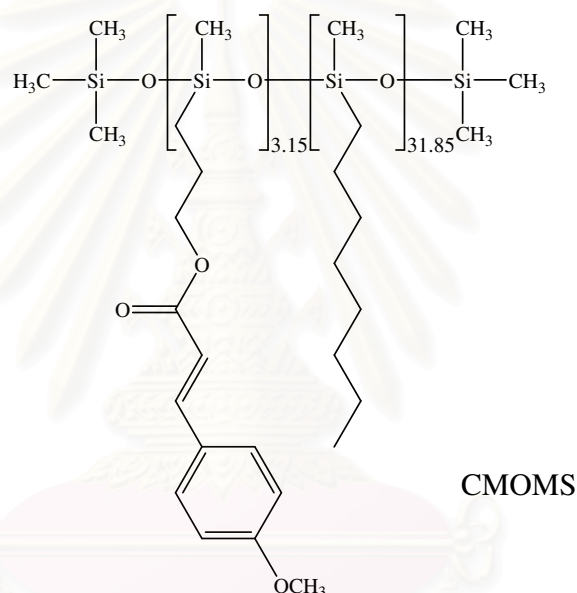
In 2005, B.I. Olvera-Martinez and coworkers [29] prepared cellulose acetate phthalate nanocapsules (polymeric nanocapsules (NCs)) containing OMC by the Emulsification-Diffusion technique. *In vivo* distribution profile through the stratum corneum of the capsules was determined by the tape-stripping technique. The penetration degree of OMC from NCs were compared to the penetration degree of OMC from nanoemulsion (NE) and oil-in-water (o/w) emulsion (EM). The results indicated that the incorporation of OMC into NE increased the penetration rate of the compound. Comparing to NE, larger size and more rigid structure of the NCs could help decrease the penetration rate of the encapsulated OMC.

1.6 Polymeric Sunscreen

The following paragraph summarizes works in which organic sunscreens have been developed into polymeric sunscreens.

A US patent number 5,250,652 [30] discloses an antisolar acrylamide polymer backbone, containing coumarins, benzothiazoles, 3-(acrylamido methylbenzylidine) DL camphor (**I**) as sunscreen moieties. The water insoluble polymers of this invention are used in leave-on applications like antisolar lotion, cream, aerosol and oil.

(**I**)
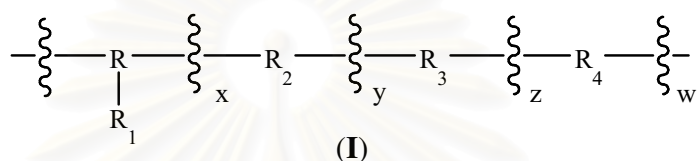
wherein :

R is a difunctional aryl or alkyl group or a difunctional straight or branched alkyl chain containing 4 to 16 carbon atoms;

R_1 is hydrogen or an aliphatic group having 1 to 20 carbons, an aryl, an alkaryl, a secondary amine, an alkali metal sulfonate, an alkali metal carboxylate, an alkyl ether, or a halogen atom;

R_2 is

R_3 is

or
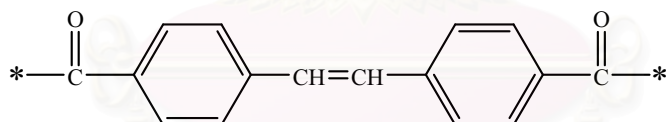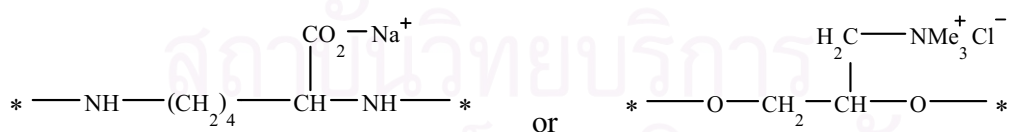
R_4 is
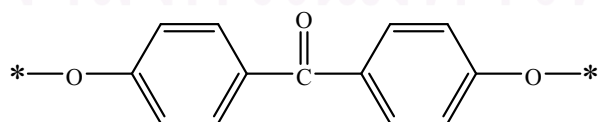
A US patent number 6,080,880 [31] described the grafting of at least one cinnamamide, benzalmalonamide or benzalmalonate group onto a short-chain silicone molecule, in particular onto a linear silicone chain comprising not more than six Si atoms (**II**, **III**). Novel compounds are obtained which obviate the drawbacks of the previously used screening agents. These novel compounds having very high-performance screening properties and very good solubility in the usual organic solvents and in particular fatty substances such as oils, as well as excellent cosmetic properties. These properties render them particularly suitable for use as sunscreens in, or for the formulation of, cosmetic compositions suited for protecting the skin and/or the hair against the deleterious effects of ultraviolet radiation.
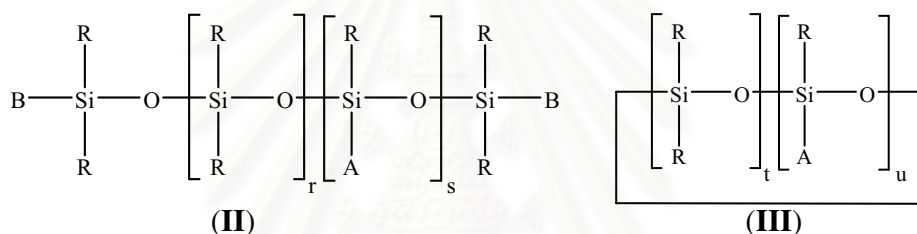
in which A is a radical of formula (a, b, c) :

(a)

(b)

(c)

in which :

the radicals R, which maybe identical or different, are each a saturated or unsaturated, linear or branched C1-C10 alkyl radical, a phenyl radical or a 3,3,3-trifluoropropyl radical, at least 80 % by number of the radicals R being methyl radicals;

the radicals B, which may be identical or different, are each a radical R or a radical A;

r is an integer ranging from 0 to 3 inclusive;

s is 0 or 1 and if s is 0, at least one of the two B is A;

u is equal to 1 or 2;

t is an integer ranging from 2 to 5 inclusive;

t+u is greater than or equal to 3

A US patent number 6,346,595 B1 [32] discloses some novel silicone compounds those contain a UV-absorber and polyethylene oxide moieties (**IV**). The dimethicone copolyol group functions not only to alter the UV absorption properties of the compounds making them acceptable UVB screens, but also modifies the solubility of the silicone compounds making them acceptable for formulation into water, silicone and oil phases.

(**IV**)

wherein :

a is an integer ranging from 0 to 2000;

b and c are an integer ranging from 1 to 20;

n is an integer ranging from 10 to 20;

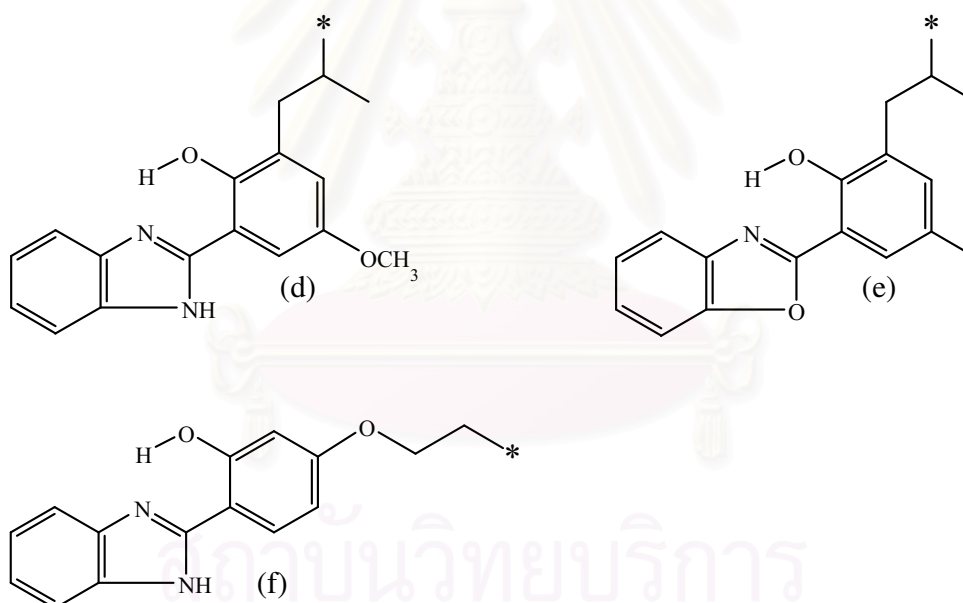d, w, x, y and z are an integer ranging from 0 to 20

A US patent number 6,376,679 B2 [33] discloses a grafting of one or more benz-x-azole (**V**, **VI**) groups on to a silicone chain. The obtained product showed excellent filtering properties in the UVA and/or UVB radiation range and provide very good solubility in the commonly used organic solvents and particularly fatty substances such as oils, as well as excellent cosmetic properties.

(**V**)   (**VI**)

in which A is a radial of formula (d, e, f) :

(d)   (e)

(f)

in which :

R designates a hydrocarbonic group saturated or unsaturated at C1-C30, a hydrocarbonic group halogenated at C1-C8, or a trimethylsilyloxy group;

B components, either identical or different, are chosen from among the R radicals and the A radical;

r is a whole number of between 0 and 50 inclusively;

s is a whole number of between 0 and 20 inclusively and if s is 0, then at least one of the B symbols is A;

u is whole number of between 1 and 6 inclusively;

t is whole number of between 0 and 10 inclusively;

t+u is equal to or greater than 3

A US patent number 7,087,692 B2 [34] involves synthesis of water-soluble polymers containing cinnamidoalkylamines and/or benzamidoalkylamines (**VII**). The polymers contain cationic centres for enhanced substantivity. When these water-soluble polymers are applied to skin, the temperature of human body and the salt content of water (in case of swimming in the sea) make them insoluble and hence do not get easily washed off either by sweat or sea water. These properties make these macromolecules useful for personal care as well as fabric care products. The synthesis of the polymer **VII** was carried out in three step, (1) synthesis of cinnamidoalkylamines and/or benzamidoalkylamines (**VIII**), (2) copolymerization of monomer **IX** and vinyl benzyl chloride and (3) functionalisation of the obtained copolymer by quaternisation using **VIII**.
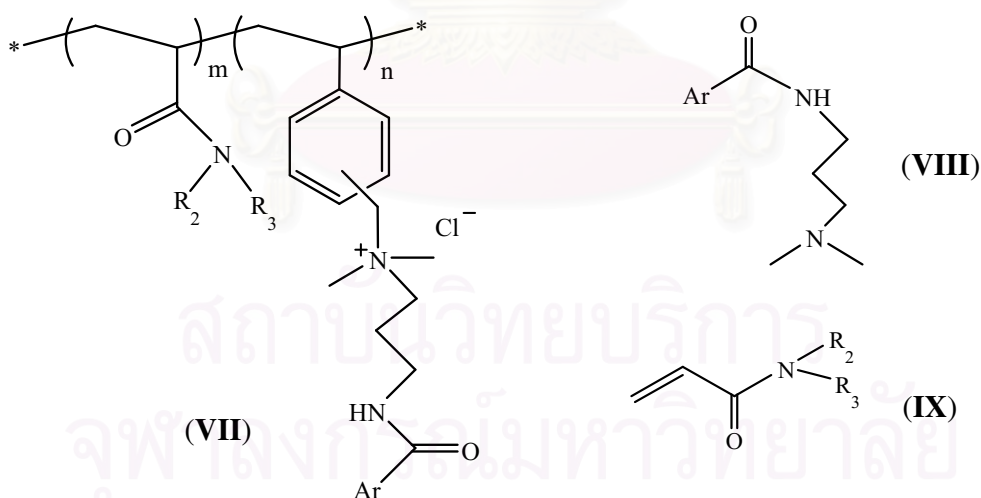
wherein :

ArCO is an UV-absorbing moiety of an organic sunscreen acid or mixtures of organic sunscreen acids selected from *p*-methoxy cinnamic acid and *p*-dimethyl amino benzoic acid;

R_2 and R_3 are selected from hydrogen, alkyl and cycloalkyl group containing from 1 to 6 carbon atoms;

m is an integer from 5 ti 9;

n is an integer between 1 to 5;

m+n is equal to 10

1.7 Polyester

Polyesters can be produced by direct esterification of a diacid with a diol or self-condensation of a hydroxyl carboxylic acid. Since polyesterification, like many step polymerization, is an equilibrium reaction, water must be continuously removed to achieve high conversions and high molecular weights.

Simple esterification is usually carried out by a well-know acid-catalyzed reaction which involves protonation of the carboxylic acid. Another acceptable method of making polyester is through acid chloride (most reactive of carboxylic acid derivatives) can be producing other derivatives. For example, direct esterification of dicarboxylic acid chloride with diol or self-condensation of hydroxyl carboxylic acid chloride to produces polyester. HCl is the inorganic by-product in all of these reactions.

The best reagents for converting carboxylic acid to acid chlorides are thionyl chloride ($SOCl_2$) and oxalyl chloride ($COCl_2$) because they form gaseous by-products which do not contaminate the product.

An example of polyesters formation through acid chloride was the work of M.Saminathan and coworkers [35]. They synthesized liquid crystalline (LCD) polymers containing azobenzone mesogen in the main chain and the unsaturated C15 hydrocarbon side chain as the pendent group. The azobenzene group was introduced by the diazo coupling reaction between cardanol and 4-aminobenzoic acid. The resulting monomers, 4-[(4-Cardanyl)azo]benzoic acid (**I**) was polymerized by self-polycondensation using thionyl chloride and pyridine to get poly[4-(4-cardanyl)azo]benzoic acid] (**II**) (**Scheme 1**).
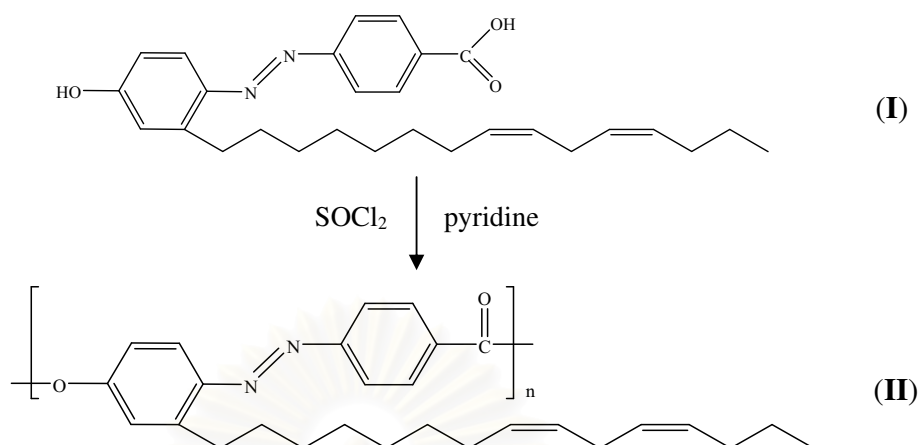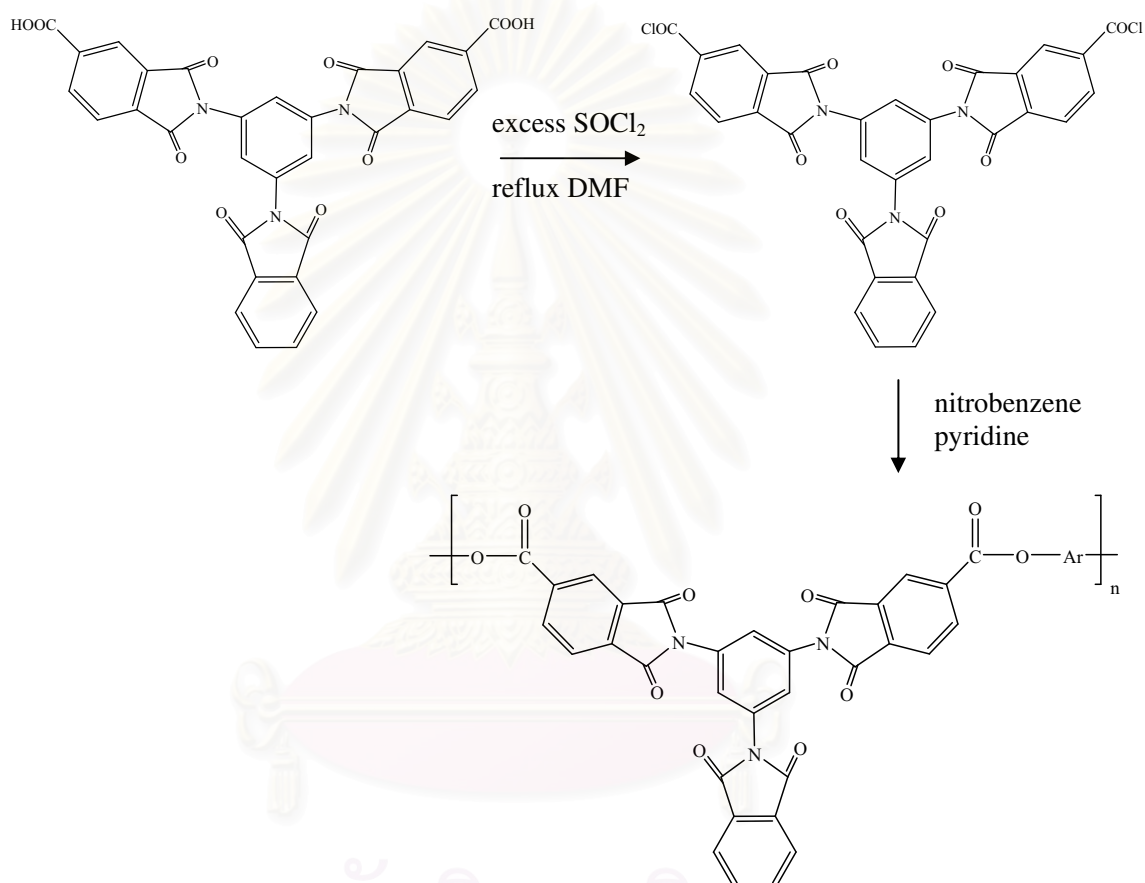
Scheme 1

In the same year, S. Jo and coworkers [36] reported a novel preparatory method of poly(ethylene glycol) (PEG) tethered to poly(propylene fumarate) (PPF). The method involved transforming carboxyl group in bis-carboxymethyl PEG (PEG-COOH) into acid chloride (using SOCl$_2$) and reacting PEG-carbonyl chloride (PEG-COCl) with PPF (**Scheme 2**).

PEG-tethered PPF
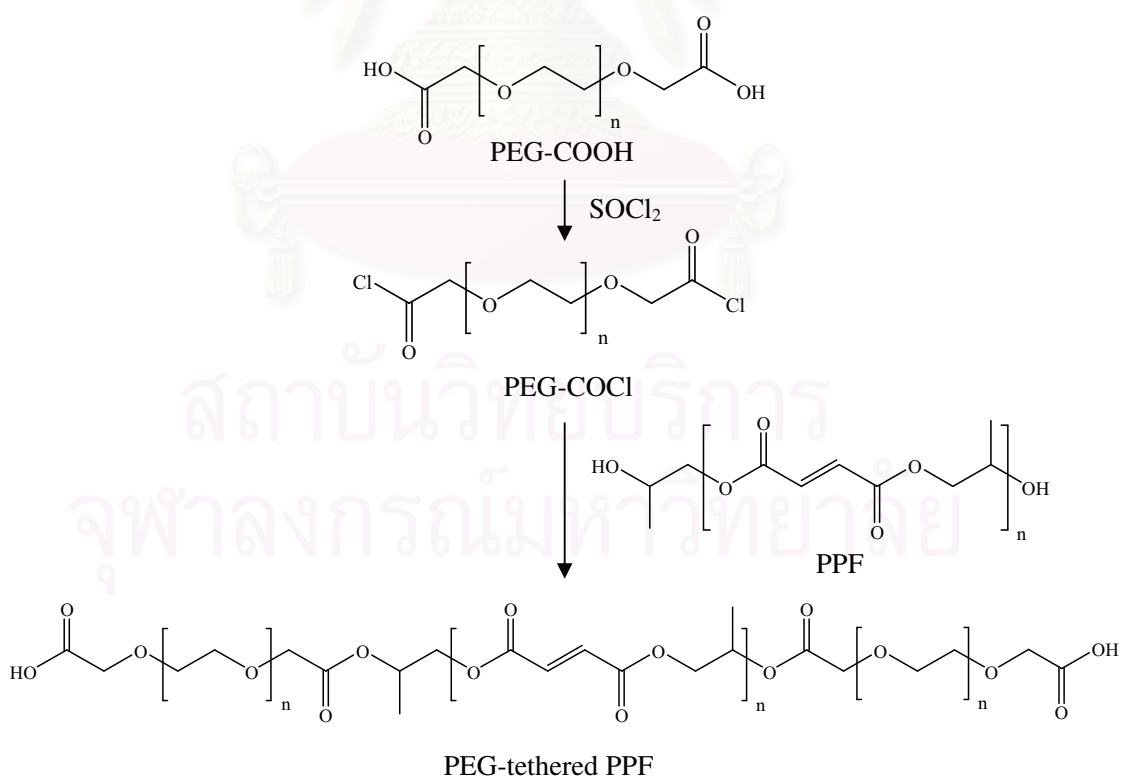
Scheme 2

In 2005, H. Benhniafar and coworkers [37] synthesised poly(ester-imide)s that exhibited high thermal stability and excellent solubility in some polar organic solvents, from a new dicarboxylic acid chloride containing three preformed imide rings with various aromatic dihydroxy compounds (Ar) using high-temperature solution poly-condensation in nitrobenzene with pyridine as hydrogen chloride trap (**Scheme 3**).

Scheme 3

1.7 Objective

The aim of this research is to 1) prepare the oligomers or polymers containing *p*-alkoxycinnamate as repeating units, 2) study UV absorption properties including molar absorptivity and photostability of the product and 3) study some physico-chemical properties such as melting point and solubility of all prepared polymers.

CHAPTER II
EXPERIMENTAL

2.1 Instruments and Experiments

Thin layer chromatography (TLC) was performed on aluminium sheets precoated with silica gel (Merck Kieselgel 60 F_{254}) (Merck KgaA, Darmstadt, Germany). Column chromatography was performed by silica gel (Merck Kieselgel 60 G) (Merck KgaA, Darmstadt, Germany). Melting points were determined with a Stuart Scientific Melting Point SMP 1 (Bibby Sterilin, Ltd., Staffordshire, UK). For UV irradiation, broad band UVA (320-400 nm) was generated by F24T12/BL/HO (PUVA) lamp (National Biological Corporation, Twinsburg, Ohio, USA) and broad band UVB (280-320 nm) was generated by FSX24T12/UVB/HO lamp (National Biological Corporation, Twinsburg, Ohio, USA). UV Irradiance was measured using UVA-400C and UVB-500C power meter (National Biological Corporation, Twinsburg, Ohio, USA).

The ^{1}H- and ^{13}C-NMR spectra were obtained in deuterated chloroform ($CDCl_3$) or deuterated dimethylsulfoxide (DMSO-d_6) with tetramethylsilane (TMS) as an internal reference using Varian Mercury NMR spectrometer which operated at 400.00 MHz for ^{1}H or 100.00 MHz for ^{13}C nuclei (Varian Company, USA). The FT-IR spectra were recorded on a Nicolet Fourier Transform Infrared spectrophotometer: Impact 410 (Nicolet Instrument Technologies, Inc. WI, USA). Molecular weights were determined by gel permeation chromatography: waters styragel HR columns, Waters 600E Multisolvent Delivery System (Waters, MA, USA). Glass transition temperature and melting temperature were determined by differential scanning calorimetry: Netzsch DSC 204 (Netzsch, Germany). UV spectra were obtained with the aids of UV 2550 UV/VIS spectrophotometer (Shimudzu Corporation, Kyoto, Japan). The UV absorbances were recorded using a quartz cell with 1 cm pathlength. Mass spectra were recorded on an Ultraflex MALDI-TOF mass spectrometer (Bruker Daltonics, MA, USA). The matrixs used were simapinic acid (*m/z* = 224.07) and 2,5-dihydroxybenzoic acid (m/z = 154.03). ESI-MS analyses were performed with Waters Micromass Quattomicro API ESCi (Waters, MA, USA). Samples were dissolved in CH_3CN and directly injected into the mass spectrometer. Transmission Electron Microscopy (TEM) was determined by JEM-

2100 (Jeol, Ltd., Japan). Particle size analysis was performed by Mastersizer S and Zetasizer nanoseries (Mulvern Instruments, UK) at the National Metal and Materials Technology Center (MTEC).

2.2 Chemicals

Solvents used in syntheses and spectroscopic works were reagent or analytical grades purchased from Labscan (Bangkok, Thailand) and Carlo Erba Reagents (Rodano, Italy). Solvents used for column chromatography were purified from commercial grade solvents prior to use by distillation. 4-Hydroxybenzaldehyde, 1,2-dibromoethane, 1,12-dibromododecane, malonic acid, polyethylene glycol (MW=200) and polyethylene glycol (MW=400) were purchased from Acros (New Jersey, USA). Potassium carbonate was purchased from Fluka Chemical Company (Buchs, Switzerland). Piperidine was purchased from Sigma (Sigma Chemical Co., Steinheirg, Germany). Standard 2-ethylhexyl-p-methoxycinnamate (EHMC) was obtained from Merck Co. Ltd. (Bangkok, Thailand).

2.3 Syntheses of Monomers
Step one:

In a 250 mL two neck round bottom flask, 4-hydroxybenzaldehyde (6.11 g, 0.05 mole) was dissolved in 70 mL of CH_3CN. Potassium carbonate and dibromoalkane were added (**Table 2.1**) and the mixture was refluxed at 78-80 °C in two neck round bottom flask attached with condenser and N_2 purge until no 4-hydroxybenzaldehyde could be detected by TLC, R_f 0.40 (50% EtOAc/Hexane (**mm2**) and R_f 0.70 (50% EtOAc/Hexane) (**mm12**) (**Scheme 2.1**). The reaction mixture was evaporated and redissolved in 100 mL CH_2Cl_2 before it was washed with 3×100 mL water. The organic solution was then dehydrated with anhydrous sodium sulfate. The solvent was then removed by rotary evaporator. The resulting product were 1,2-(bis(4-(formylphenoxy))ethane (**mm2**) and 1,12-(bis(4-(formylphenoxy))dodecane) (**mm12**). The product was further purified by a silica gel column using 40:60 (v/v) CH_2Cl_2:hexane (for **mm2**) and 60:40 (v/v) CH_2Cl_2:hexane (for **mm12**) as an eluent.
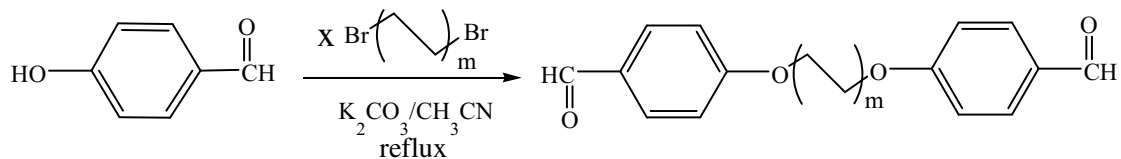
m = 1,6

Scheme 2.1

**Table 2.1** Amount of potassium carbonate and dibromoalkane used in the reactions

Cpds	Grams	Mole	m	Mole equivalent of x
1,2-dibromoethane	13.15	0.07	1	3
K_2CO_3	9.67	0.07	-	-
1,12-dibromododecane	4.70	0.025	6	1
K_2CO_3	6.91	0.05	-	-

*1,2-(bis(4-(formylphenoxy))ethane) (**mm2**)* : white solid (68%), R_f 0.40 (50% EtOAc/ Hexane), ^{1}H-NMR (CDCl$_3$) δ (ppm) : 9.91 (s, 2H, Ar-**CHO**), 7.88-7.86 (d, 4H, Ar-**H**, J = 8.58 Hz), 7.07-7.05 (d, 4H, Ar-**H**, J = 8.58 Hz) and 4.45 (s, 4H, -**CH₂**-O-Ar) (**Figure B.1**)

*1,12-(bis(4-(formylphenoxy))dodecane) (**mm12**)* : white solid (68%), R_f 0.70 (50% EtOAc/Hexane), ^{1}H-NMR (CDCl$_3$) δ (ppm) : 9.92 (s, 2H, Ar-**CHO**), 7.88-7.86 (d, 4H, Ar-**H**, J = 8.58 Hz), 7.04-7.02 (d, 4H, Ar-**H**, J = 8.58 Hz), 4.08 (s, 4H, -**CH₂**-O-Ar) and 1.85-1.34 (br, 20H, -**CH₂**-) (**Figure B.2**)

Step two:

The obtained **mm2** (13.50 g, 0.05 mole) and **mm12** (20.50 g, 0.05 mole) were dissolved in pyridine and malonic acid (20.80 g, 0.20 mole) and piperidine (8.51 g, 0.10 mole) were added. The mixture was refluxed at 78-80 °C in two neck round bottom flask attached with condenser for 74 and 79 hours, respectively (**Scheme 2.2**). After being cooled the reaction mixture was evaporated and acidified with 200 mL of 2 M HCl. The solid was separated by suction filtration and washed with water.
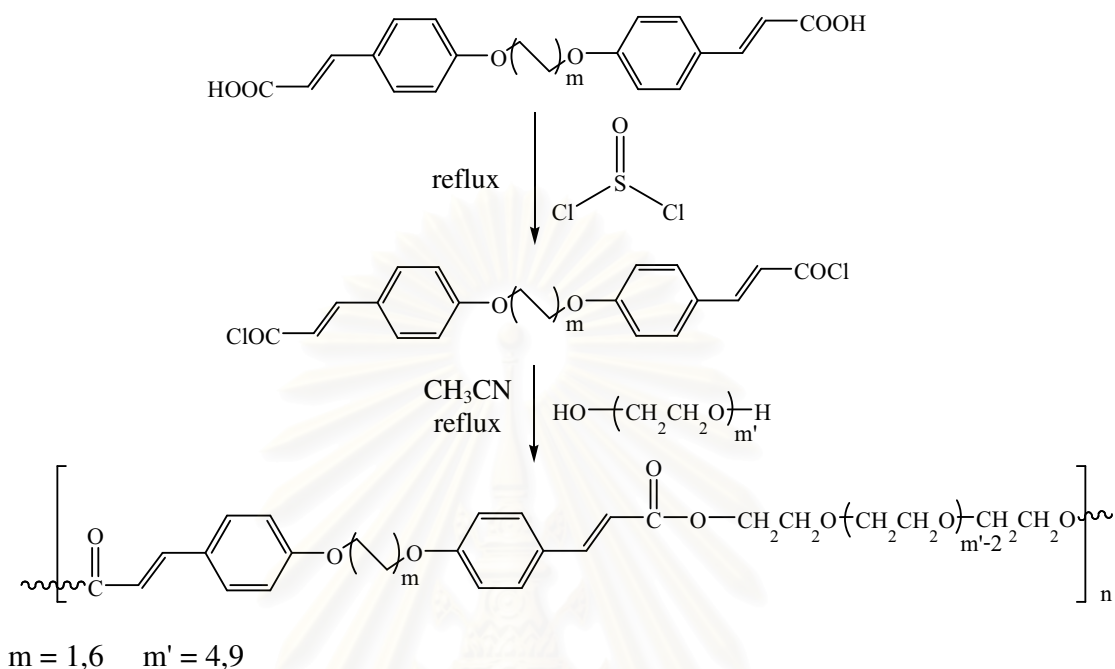
Scheme 2.2

m = 1,6
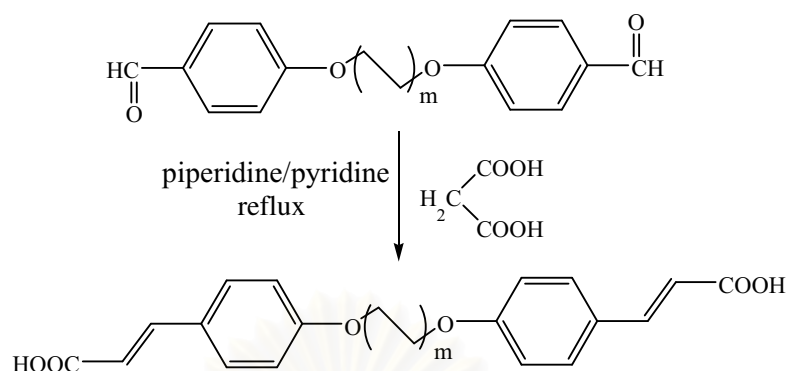
1,2-(bis(4-(2-carboxyvinyl)phenoxy))ethane (M2) : white solid (70%), m.p. 310-315 °C, IR (KBr, cm^{-1}) : 3200-2400, 1677, 1599, 1509 and 1241 (**Figure B.5**); ^{1}H-NMR (DMSO-d_6) δ (ppm) : 12.24 (s, 2H, -CO**OH**), 7.59-7.57 (d, 4H, Ar-**H**, J = 8.58 Hz), 7.50-7.46 (d, 2H, Ar-C**H**=, J = 16.38 Hz), 6.97-6.95 (d, 4H, Ar-**H**, J = 8.58 Hz), 6.34-6.30 (d, 2H, Ar-C**H**=, J = 16.38 Hz), 4.31 (s, 4H, -C**H₂**-O-Ar) (**Figure B.3**); ^{13}C-NMR (DMSO-d_6) δ (ppm) : 168.3 (-**C**OOH), 160.4 (-**C**-), 144.1 (Ar-**C**H=), 130.4 (=**C**H-) (aromatic carbons), 127.5 (-**C**-), 117.1 (=**C**H-COOH), 115.3 (=**C**H-) (aromatic carbons) and 66.9 (-**C**H₂-O-Ar) (**Figure B.4**)

1,12-(bis(4-(2-carboxyvinyl)phenoxy))dodecane (M12) : white solid (60%), m.p. 202-205 °C, IR (KBr, cm^{-1}) : 3200-2400, 1671, 1593, 1511 and 1246 (**Figure B.8**); ^{1}H-NMR (DMSO-d_6) δ (ppm) : 7.59-7.57 (d, 4H, Ar-**H**, J = 8.58 Hz), 7.52-7.48 (d, 2H, Ar-C**H**=, J = 16.38 Hz), 6.93-6.91 (d, 4H, Ar-**H**, J = 8.58 Hz), 6.36-6.32 (d, 2H, Ar-C**H**=, J = 16.38 Hz), 3.97 (s, 4H, -C**H₂**-O-Ar), 1.68-1.24 (br, 20H, -C**H₂**-) (**Figure B.6**); ^{13}C-NMR (DMSO-d_6) δ (ppm) : 168.3 (-**C**OOH), 160.8 (-**C**-), 144.0 (Ar-**C**H=), 130.3 (=**C**H-) (aromatic carbons), 127.4 (-**C**-), 117.0 (=**C**H-COOH), 115.2 (=**C**H-) (aromatic carbons), 68.0 (-**C**H₂-O-Ar) and 29.4-25.9 (-**C**H₂-) (**Figure B.7**)

2.4 Syntheses of Copolymers

Scheme 2.3

2.4.1 Condensation polymerization using thionyl chloride in **M2**

Monomer (**M2**) (0.354 g, 1 mmole) and excess freshly distilled thionyl chloride (15 mL) were refluxed at 78-80 °C in two necked round bottom flask attached with a condenser and drying tube containing anhydrous sodium sulfate for 3 hours. Unreacted thionyl chloride was removed under reduced pressure to give 1,2-(bis(4-(2-chlorocarbonyl vinyl)phenoxy))ethane. Then poly(ethylene glycol) MW~200 (0.02g, 1 mmole) was added and the mixture was then reflux at 80°C for 28 hours in 20 mL (for **P2-PEG200** and **P2-PEG400**) or 5 mL (for **P2-PEG400C**) CH₃CN (**Scheme 2.3**). The reaction mixture was cooled to room temperature, then evaporated and redissolved in 50 mL EtOAc before it was washed with 3×50 mL water. Water was removed from EtOAc using anhydrous sodium sulfate. The solvent was then removed by rotary evaporation.

Poly((1,2-(bis(4-(2-carboxyvinyl)phenoxy))ethane)-*co*-(poly(ethylene glycol)200)) *(P2-PEG200)* : yellow wax, T_g = -18.8 °C, T_m = 91.1 °C (**Figure B.12**), IR (NaCl, cm⁻¹) :

1705, 1599, 1510 and 1244 (**Figure B.11**), ^{1}H-NMR (CDCl$_3$) δ (ppm) : 7.67-7.63 (Ar-**CH**=, J = 15.60 Hz), 7.49-7.46 (Ar-**H**), 6.96-6.93 (Ar-**H**), 6.37-6.33 (Ar-**CH**=, J = 15.60 Hz), 4.36-4.34 (-**CH$_2$**-O-Ar, -COO-**CH$_2$**-) and 3.78-3.63 (-**CH$_2$**-O-) (**Figure B.9**)

Poly((1,2-(bis(4-(2-carboxyvinyl)phenoxy))ethane-*co*-(poly(ethylene glycol)400)) *(P2-PEG400* and *P24-PEG400C)* : yellow oil, T$_g$ = -20.1 °C (**Figure B.1**7), IR (NaCl, cm^{-1}) : 3700-3300, 1705, 1603, 1514 and 1244 (**Figure B.1**6), ^{1}H-NMR (CDCl$_3$) δ (ppm) : 7.68-7.64 (Ar-**CH**=, J = 15.60 Hz), 7.50-7.48 (Ar-**H**, J = 7.8 Hz), 6.96-6.94 (Ar-**H**, J = 7.8 Hz), 6.38-6.34 (Ar-**CH**=, J = 15.6 Hz), 4.38-4.34 (-**CH$_2$**-O-Ar, -COO-**CH$_2$**-) and 3.79-3.60 (-**CH$_2$**-O-) (**Figure B.14**)

2.4.2 Condensation polymerization using thionyl chloride in **M12**

Monomer (**M12**) (0.494 g, 1 mmole) and excess freshly distilled thionyl chloride (15 mL) were refluxed at 78-80 °C in two necked round bottom flask attached with a condenser and drying tube containing anhydrous sodium sulfate for 3 hours. Unreacted thionyl chloride was removed under reduced pressure, to give 1,12-(bis(4-(2-chlorocarbonylvinyl)phenoxy))dodecane and then poly(ethylene glycol) MW~400 (0.40 g, 1 mmole) was added and the mixture was then reflux at 80°C for 28 hours in 20 mL CH$_3$CN. The reaction mixture was cooled to room temperature, then evaporated and redissolved in 50 mL EtOAc before it was washed with 3×50 mL water. Waters was removed from EtOAc using anhydrous sodium sulfate. The solvent was then removed by rotary evaporation.

Poly((1,12-(bis(4-(2-carboxyvinyl)phenoxy))dodecane)-*co*-(poly(ethylene glycol)400)) *(P12-PEG400)* : yellow wax, T$_g$ = -50.7 °C, T$_m$ = 79.0 °C (**Figure B.23**), IR (NaCl, cm^{-1}) : 3700-3300, 1709, 1603, 1501 and 1248 (**Figure B.22**), ^{1}H-NMR (CDCl$_3$) δ (ppm) : 7.68-7.64 (Ar-**CH**=, J = 15.60 Hz), 7.47-7.45 (Ar-**H**, J = 7.8 Hz), 6.90-6.88 (Ar-**H**, J = 7.8 Hz), 6.36-6.32 (Ar-**CH**=, J = 15.60 Hz), 4.37-4.34 (-**CH$_2$**-O-Ar), 3.99-3.96 (-COO-**CH$_2$**-), 3.79-3.60 (-**CH$_2$**-O-) and 1.82-1.22 (-**CH$_2$**-) (**Figure B.20**)

2.5 General Procedure for Molar Absorptivity Measurements

Test compounds were dissolved in dimethylformamide to the concentration of about 1 mg/5 mL (for monomer) or 2 mg/5 mL (for polymer). The resulting stock solution was then diluted to appropriate concentrations using dimethylformamide. The UV absorbance of each final dilution was recorded by scanning wavelengths between 200 and 800 nm. The molar absorptivity (ε) at the wavelength of maximum absorbance (λ_{max}) was calculated using Beer's law:

$$A = \varepsilon bc$$

Where A is absorbance

b is the cell path length (1 cm)

c is the concentration of the absorbing species in mole per litre

2.6 General Procedure for Photostability Test

The photostability tests were performed in dimethylformamide. The solutions (12 ppm) were divided into two parts. One part was kept away from light (covered with foil) at room temperature (dark sample) while at the same temperature the other was irradiated by artificial UV lamp (irradiated sample) at 3.0 mW/cm^2 UVA and 0.25 mW/cm^2 UVB. Then UV absorption profile of each sample was acquired using UV/Vis spectrometer. The absorbance of irradiated sample at various irradiant times was compared to those of dark samples.

The calculation of percent relative absorbance of each irradiated sample was done using the following equation.

$$\text{Percent of relative absorbance} = \frac{\text{Absorbance of irradiated sample at time x}}{\text{Absorbance of dark sample (starting time)}} \times 100$$

2.7 Syntheses of Nano/microparticles

Twenty mg of **P2-PEG400** or **P12-PEG400** was dissolved in 5 mL of acetone solution. The solution was put into a dialysis bag and placed into a beaker containing 800 mL of deionized water. The solution was dialyzed for three days with 3×800 mL changes of deionized water.

CHAPTER III
RESULTS AND DISCUSSION

In this thesis, an oligomeric/polymeric material with chromophoric structural component that can absorb UV light was the synthesis goal. To do so, monomeric units with UV absorption property were created. Since cinnamate is class of UV filtering agent used world-wide, polymers based on cinnamate monomeric units were pursued in this work.

3.1 Syntheses of Monomers

The syntheses of cinnamate-based-monomeric units were done in two steps.
Step one : alkylation between two mole equivalents of 4-hydroxybenzaldehyde and various mole equivalents of dibromoalkane (**Table 3.1**) using two mole equivalents of potassium carbonate as a catalyst. 1,2-Dibromoethane and 1,12-dibromododecane were used and the resulting products were 1,2-(bis(4-(formylphenoxy))ethane (**mm2**) and 1,12-(bis(4-(formylphenoxy))dodecane) (**mm12**).

Table 3.1 Reaction conditions of **mm2** and **mm12**
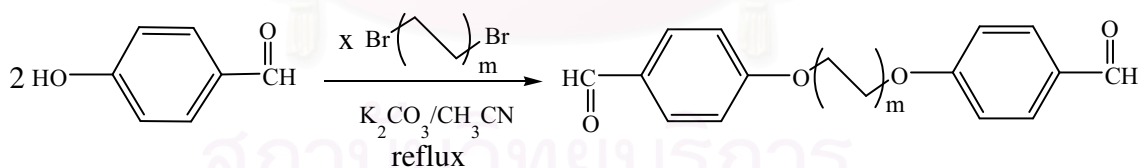
m = 1,6

Products	$2 \times m$	Mole equivalent of dibromoalkane (x)	Reaction time (hour)	% yield
1,2-(bis(4-(formylphenoxy)) ethane) ; (**mm2**)	2	3	74	68
1,12-(bis(4-(formylphenoxy)) dodecane) ; (**mm12**)	12	2	79	68

Step two : Knovenagel condensation between one mole equivalent of the products from step one (dialdehyde) and five mole equivalents of malonic acid, using two mole equivalents of piperidine as a catalyst (**Scheme 2.2**).

The structures of the obtained monomers were characterized using various spectroscopic techniques including ^{1}H-NMR, ^{13}C-NMR and IR spectroscopy (see **Appendix B**). All spectroscopic data confirmed the structures of 1,2-(bis(4-(2-carboxyvinyl)phenoxy))ethane (**M2**) and 1,12-(bis(4-(2-carboxyvinyl)phenoxy)) dodecane (**M12**). It can be seen that **M2** and **M12** possess similar solubility properties (**Table 3.2**) resulting from the small influences of their chemical structures at the alkyl chain spacer between the two benzene rings.

Table 3.2 Solubility property of the synthesized monomers

Compounds	M2	M12
pyridine	+	+
dimethylformamide	+	+
dimethylsulfoxide	+	+*
ethanol	-	-
methanol	-	-
acetone	-	-
ethyl acetate	-	-
tetrahydrofuran	-	-
chloroform	-	-
dichloromethane	-	-
diethyl ether	-	-
toluene	-	-
hexane	-	-

+ soluble at 2 mg/mL   * after heating (60 °C)

All two monomers show similar UVB absorption band (**Figure 3.1**). This agrees well with the fact that the two monomers contain the same chromophoric moieties.
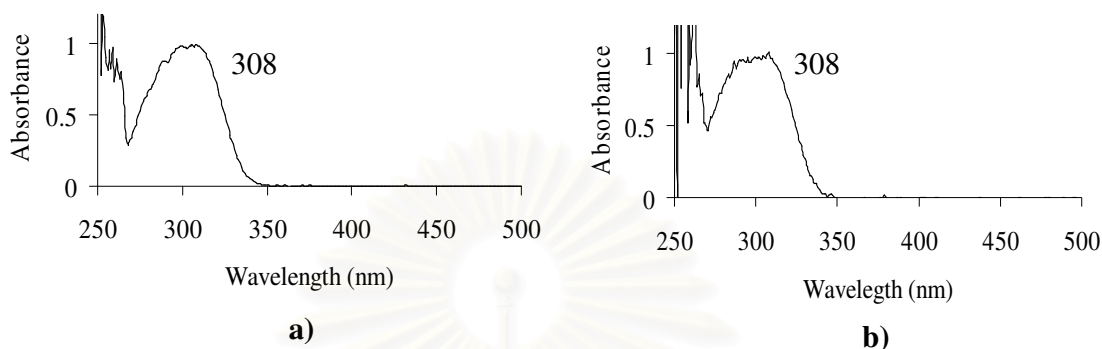
Figure 3.1 UV spectra of a) **M2** and b) **M12**

By plotting a graph between absorbance (at λ_{max}) and concentrations of each monomer sample, a linear relationship was obtained with its slope represented the molar absorptivity (ε) of the monomer. The two monomers give comparable ε and λ_{max} (**Table 3.3**). The ε values of both monomers are about twice the value of *p*-methoxycinnamic acid (22,000 $M^{-1}cm^{-1}$). This is expected because each molecule of **M2** and **M12** contains two cinnamic units.

Table 3.3 UV spectral data of monomers in dimethylformamide

Compound	λ_{max}	ε ($M^{-1}cm^{-1}$)
M2	308	44000
M12	308	45000

3.2 Syntheses of Copolymers

M2 and **M12** were subjected to copolymerization with polyethylene glycol (**PEG**) (**Scheme 2.3**) in order to create polymers with improved solubility.

The monomer **M2** was subjected to condensation polymerization by esterification reaction with **PEG200** (**PEG** with MW of 200) and **PEG400** (**PEG** with MW of 400) through acid chloride method. The obtained polymers (**P2-PEG200** and **P2-PEG400**)

were subjected to ^{1}H-NMR and IR spectroscopic analyses. ^{1}H-NMR spectrum of **P2-PEG200** (**Figure B.9**) shows -**CH$_2$**-O- resonances at ~3.7 ppm, indicating the presence of PEG moieties. Although both **M2** and **P2-PEG400** give ^{1}H-NMR signals at ~4.3 ppm (-**CH$_2$**-O-Ar- for **M2** and -**CH$_2$**-O-Ar and -COO-**CH$_2$**- for **P2-PEG200**), integration of the ~4.3 ppm signals in the polymer doubles that of the monomer. This confirms successful esterification reaction.

Similar to **P2-PEG200**, the ^{1}H-NMR spectrum of **P2-PEG400** (**Figure B.13**) shows -**CH$_2$**-O- and -COO-**CH$_2$**- resonances at ~3.7 and ~4.3 ppm, indicating the presence of polyethylene oxide. Although both **P2-PEG200** and **P2-PEG400** give ^{1}H-NMR signals at ~4.3 ppm (-COO-**CH$_2$**- for **P2-PEG200** and **P2-PEG400**), integration of the ~4.3 ppm signals in the **P2-PEG400** doubles that of the **P2-PEG200**. This confirms successful esterification reaction between **M2** and **PEG**.

This obvious change in ^{1}H-NMR together with molecular weight information from gel filtration ($\overline{\text{M}}$n of **P2-PEG200 =** 2100 and **P2-PEG400 =** 2600) confirm that esterification has taken place.

The shift of carbonyl signal from 1677 cm^{-1} in **M2** IR spectrum to 1705 cm^{-1} in **P2-PEG200** and **P2-PEG400** spectrum indicates the presence of ester functional group. This C=O stretching vibration of the **P2-PEG200** and **P2-PEG400** is lower than regular carbonyl ester because of the conjugation. The disappearance of broad absorption at 3200-2400 cm^{-1} indicated complete change of carboxylic acid into ester functionality (**Figure B.11** and **B.15**).

Similar to **M2**, the monomer **M12** was subjected to condensation polymerization by esterification reaction with **PEG400** using thionyl chloride. The obtained polymer (**P12-PEG400**) was subjected to ^{1}H-NMR and IR spectroscopic analyses. The ^{1}H-NMR spectrum of **P12-PEG400** (**Figure B.18**) shows -**CH$_2$**-O- and -COO-**CH$_2$**- resonances at ~3.7 and ~3.9 respectively, indicating the presence of polyethylene oxide chain.

The shift of carbonyl signal in IR spectrum of **M12** from 1671 cm^{-1} to 1709 cm^{-1} for **P12-PEG200** indicated the presence of ester functional group. The disappearance of broad absorption at 3200-2400 cm^{-1} indicated complete change of carboxylic acid into ester functionality (**Figure B.20**).

The progress of the polymerization reaction was followed by analyzing $\overline{M}n$ of the product obtained at various reaction times, using gel filtration. The growths of the polymer are depicted in **Figure 3.2**.
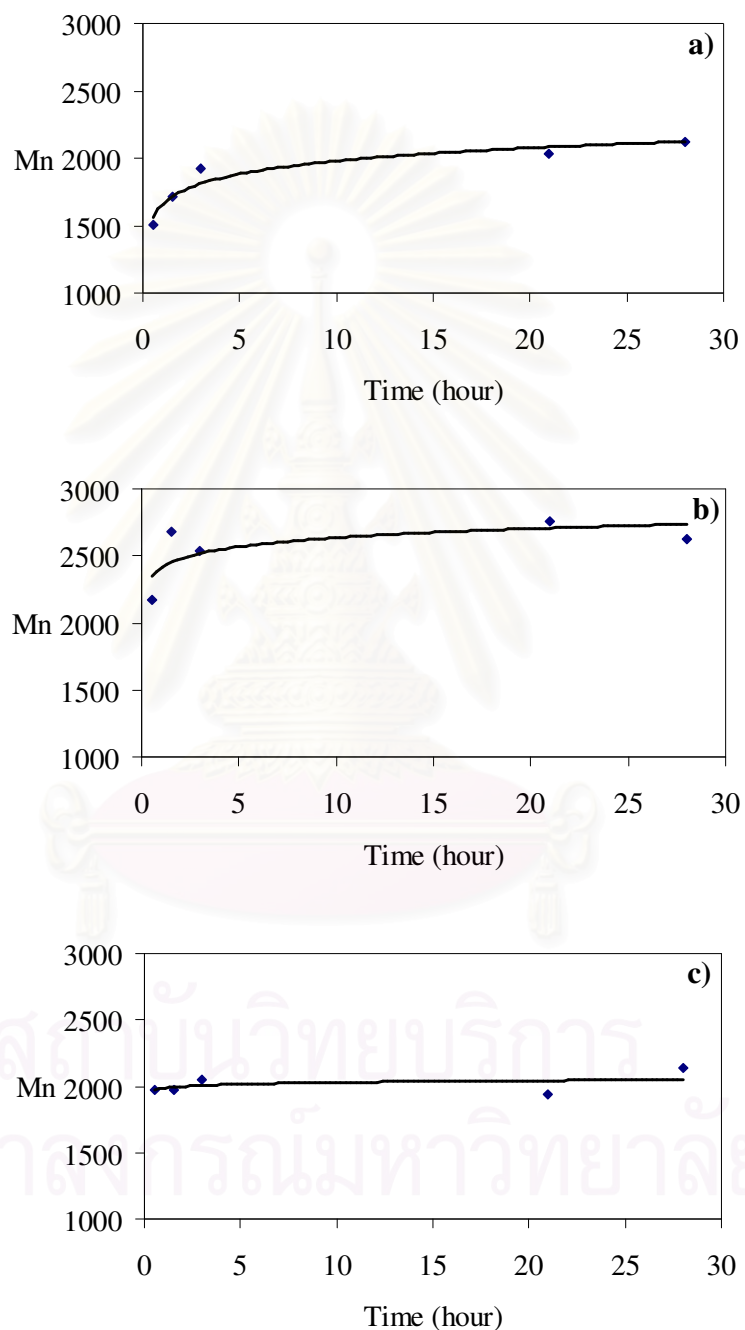

Figure 3.2 Number average molecular weight of products obtained at various reaction times; a) **P2-PEG200** b) **P2-PEG400** and c) **P12-PEG400**

The polymerizations completed within a few hours and the number average molecular weight ($\overline{M}n$) for **P2-PEG200**, **P2-PEG400** and **P12-PEG400** are 2100, 2600 and 2100 respectively.

Upon varying concentrations during condensation, the results show the $\overline{M}n$ from GPC analyses to be 2600 and 4800 for **P2-PEG400** and **P2-PEG400C** respectively (**Figure 3.3**). These results indicated that polymerization at higher concentration of monomer gave polymeric product with higher $\overline{M}n$. It was speculated that in dilute solutions, intramolecular reaction may interfere and give rise to cyclizations. These cyclizations were confirmed by mass spectrometry. MALDI-TOF MS spectra of **P2-PEG200** showed the formation of cyclic compounds and oligomeric compounds
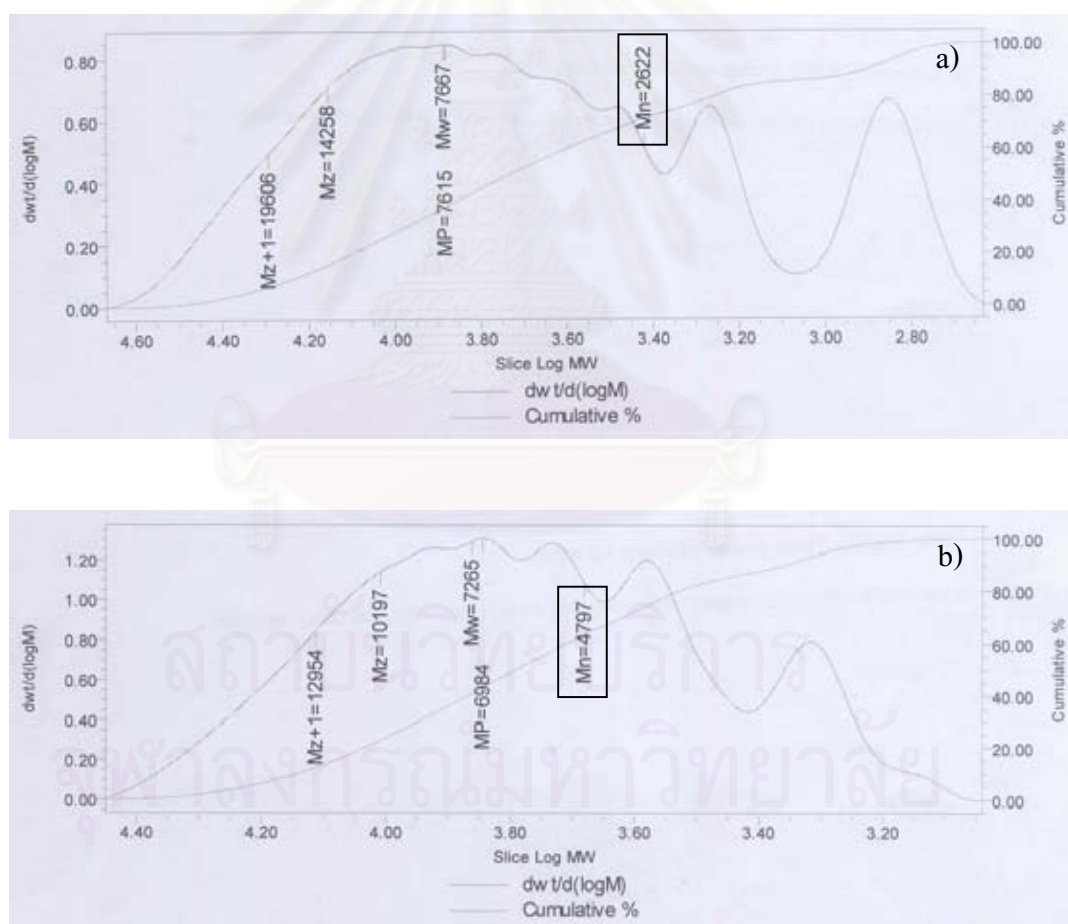
Figure 3.3 GPC spectra of a) **P2-PEG400** and b) **P2-PEG400C**

(**Figure 3.4** and **Table 3.4**). In **P2-PEG400** and **P12-PEG400**, MALDI-TOF MS spectra showed only the formation of cyclic compounds (**Figur**e **3.5-3.6** and **Table 3.5-3.6**). This indicated predominated cyclized oligomeric **P2-PEG400** and **P12-PEG400**. This was also confirmed by the lack of -COOH functionality at 2300-3600 cm^{-1} in the FT-IR spectra of both oligomers (**Figure B.16** and **22**).
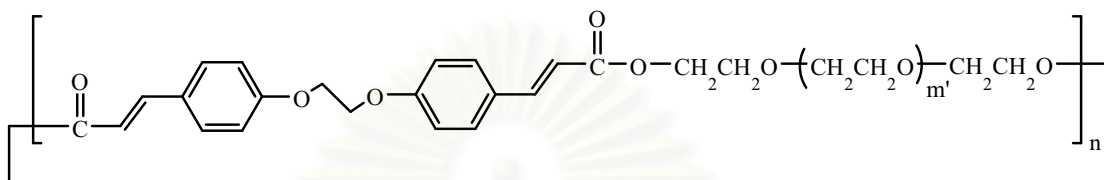
at   m' = 1 mass of polymeric unit = 468,   m' = 3 mass of polymeric unit = 556
      m' = 2 mass of polymeric unit = 512
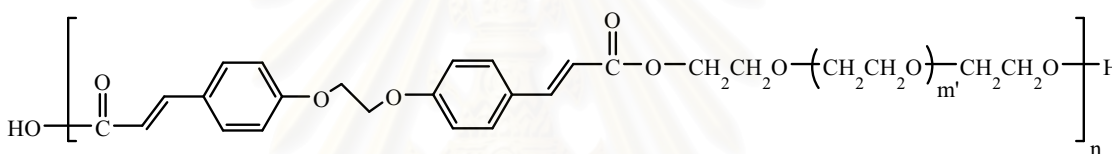
at   m' = 1 mass of polymeric unit = 486,   m' = 3 mass of polymeric unit = 574
      m' = 2 mass of polymeric unit = 530

Figure 3.4 Oligomeric structures and mass of polymeric unit of **P2-PEG200** at n = 1 : top = cyclic structure, bottom = open chain structure

Table 3.4 Masses of the cyclized and linear oligomers of **P2-PEG200** at n = 1 as determined by MALDI-TOF MS (calculated values are indicated in the brackets)

Cpds	m'	Detected m/z (or cyclized structures)	Detected m/z[a] (or open chain structures)
P2-PEG200	m'=1	467.72 (468)	485.65 (486)
	m'=2	511.66 (512)	529.60 (530)
	m'=3	555.61 (556)	573.53 (574)

[a] MALDI-TOF MS
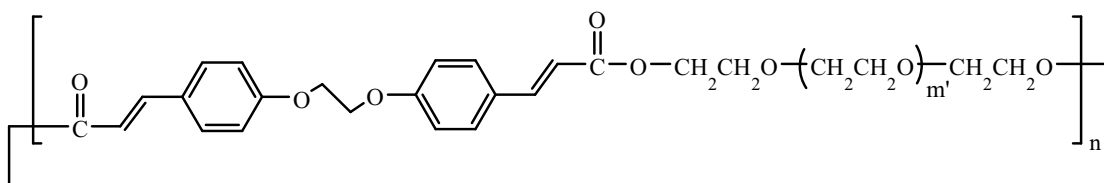
at $m' = 5$ mass of polymeric unit = 644, $m' = 8$ mass of polymeric unit = 776

       $m' = 6$ mass of polymeric unit = 688, $m' = 9$ mass of polymeric unit = 820

       $m' = 7$ mass of polymeric unit = 723
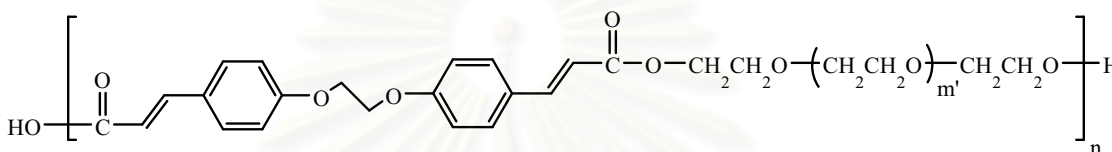
at $m' = 5$ mass of polymeric unit = 662, $m' = 8$ mass of polymeric unit = 794

       $m' = 6$ mass of polymeric unit = 706, $m' = 9$ mass of polymeric unit = 838
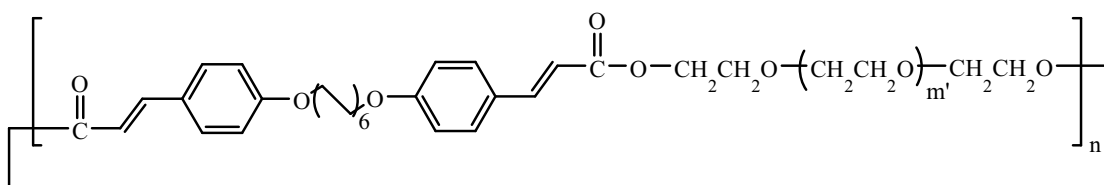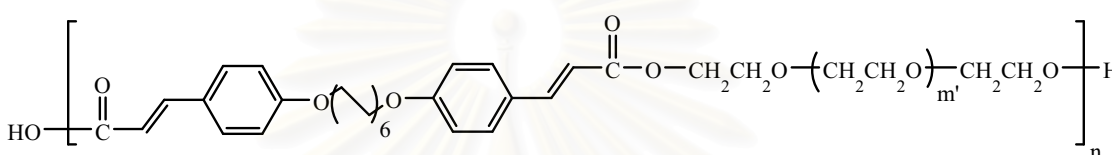
       $m' = 7$ mass of polymeric unit = 750

Figure 3.5 Oligomeric structures and mass of polymeric unit of **P2-PEG400** at $n = 1$: top = cyclic structure, bottom = open chain structure

Table 3.5 Masses of the cyclized and linear oligomers of **P2-PEG400** at $n = 1$ as determined by MALDI-TOF MS and ESI-MS (calculated values are indicated in the brackets)

Cpds	m'	Detected m/z[a] (or cyclized structures)	Detected m/z[b] (or cyclized structures)	Detected m/z[a] (or open chain structures)
P2-PEG400	$m'=5$	644.48 (644)	677.25 (677)	- (662)
	$m'=6$	688.41 (688)	721.36 (721)	- (706)
	$m'=7$	732.34 (732)	765.39 (765)	- (750)
	$m'=8$	776.27 (776)	809.40 (809)	- (794)
	$m'=9$	820.20 (820)	853.54 (853)	- (838)

[a] MALDI-TOF MS   [b] ESI-MS, m/z = [MH+EtOH]$^+$

at   m' = 5 mass of polymeric unit = 784,   m′ = 8 mass of polymeric unit = 916

m′ = 6 mass of polymeric unit = 828,   m′ = 9 mass of polymeric unit = 960

m′ = 7 mass of polymeric unit = 872

at   m' = 5 mass of polymeric unit = 802,   m' = 8 mass of polymeric unit = 934

m' = 6 mass of polymeric unit = 846,   m' = 9 mass of polymeric unit = 978

m' = 7 mass of polymeric unit = 890

Figure 3.6 Oligomeric structures and mass of polymeric unit of **P12-PEG400** at n = 1 : top = cyclic structure, bottom = open chain structure

Table 3.6 Masses of the cyclized and linear oligomers of **P12-PEG400** at n = 1 as determined by MALDI-TOF MS (calculated values are indicated in the brackets)

Cpds	m′	Detected m/z (or cyclized structures)	Detected m/z[a] (or open chain structures)
P12-PEG400	m′=5	784.30 (784)	- (802)
	m′=6	828.22 (828)	- (846)
	m′=7	872.15 (872)	- (890)
	m′=8	916.09 (916)	- (934)
	m′=9	960.01 (960)	- (978)

[a] MALDI-TOF MS

The absorption properties (λ_{max} and ε) of all polymers are reported in **Table 3.7**. The three polymers show similar UVB absorption band (**Figure 3.7**). This agrees well with the fact that all three polymers contain similar chromophoric moiety.

Table 3.7 UV spectral data of the polymeric products in dimethylformamide

Compound	λ_{max}	ε ($M^{-1}cm^{-1}$)*
P2-PEG200; yellow wax	311	51000
P2-PEG400; yellow oil	311	55000
P12-PEG200; yellow wax	311	54000

* per monomeric unit
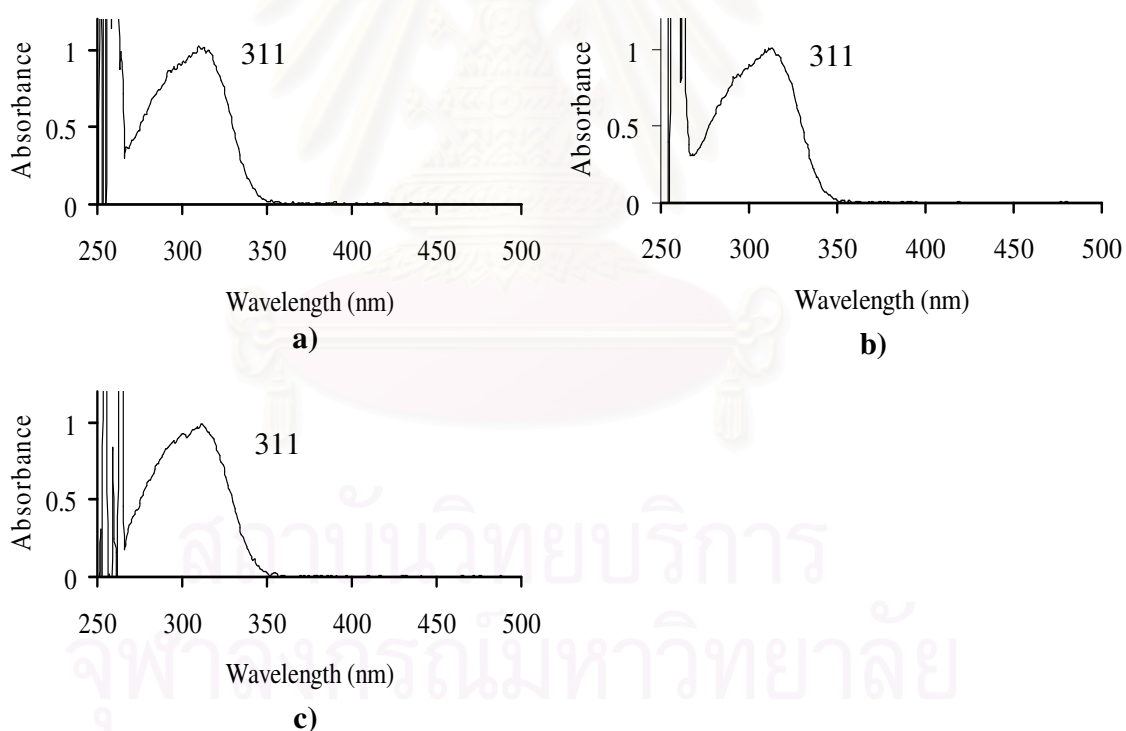
Figure 3.7 UV spectra of a) **P2-PEG200,** b) **P2-PEG400** and c) **P12-PEG400** in dimethylformamide

The three polymers are soluble in various organic solvents (**Table 3.8**) thus applications of the polymers are possible.

Table 3.8 Solubility of the synthesized polymers

Solvent	**P2-PEG200**	**P2-PEG400**	**P12-PEG400**
dimethylformamide	+	+	+
dimethylsulfoxide	+	+	+
water	-	-	-
acetonitrile	+	+	+
ethanol	-	-	-
methanol	-	-	-
acetone	+	+	+
ethyl acetate	+	+	+
tetrahydrofuran	+	+	+
chloroform	+	+	+
dichloromethane	+	+	+
diethyl ether	-	-	-
toluene	-	-	-
hexane	-	-	-
DC200[a]	-	-	-
DC245[b]	-	-	-
DC556[c]	-	-	-
DC2502[d]	-	-	-

+ soluble in 2 mg/mL

- insoluble in 2 mg/mL

[a] linear polydimethylsiloxane polymers

[b] cyclopentasiloxane

[c] phenyl trimethicone

[d] cetyl dimethicone

3.3 Photostability Test
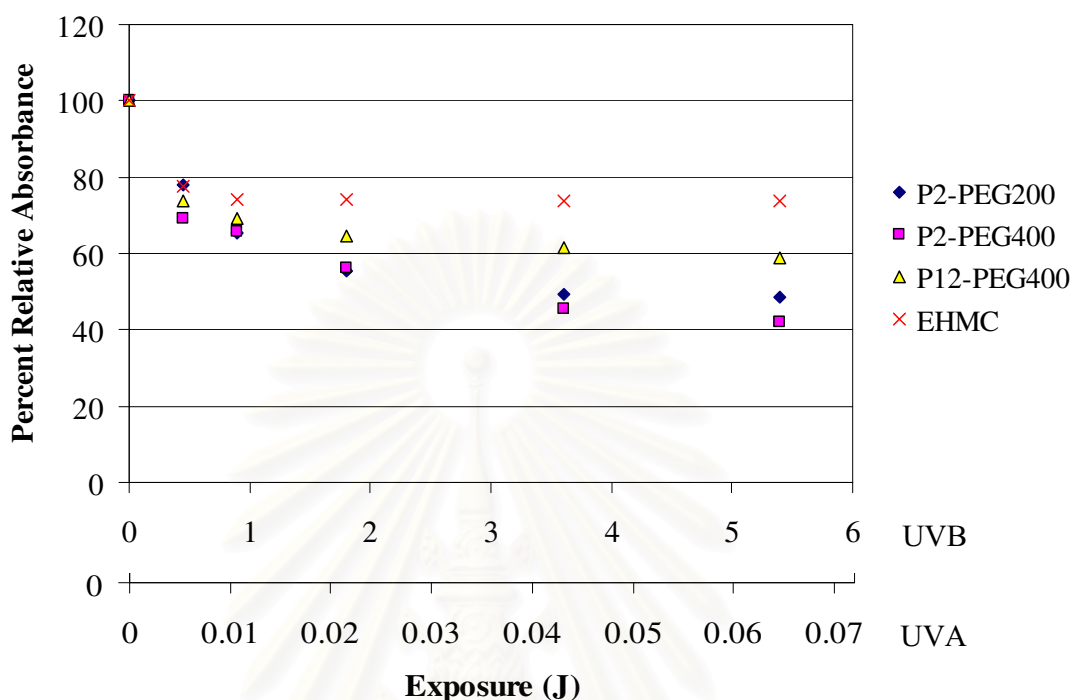
Figure 3.8 Photostability of 2-ethylhexyl-*p*-methoxycinnamate (EHMC), **P2-PEG200**, **P2-PEG400** and **P12-PEG400** in dimethylformamide. The light intensities were 3.0 mW/cm^2 for UVA and 0.25 mW/cm^2 for UVB

Three synthesized polymeric UV-filter **P2-PEG200**, **P2-PEG400** and **P12-PEG400** were subjected to photostability test. The tests were carried out in dimethylformamide. The test solution was irradiated with 3.0 mW/cm^2 UVA and 0.25 mW/cm^2 UVB for 30, 60, 120, 240 and 360 min which correspond to 0.0054, 0.0108, 0.0216, 0.0432 and 0.0648 J UVA and 0.45, 0.90, 1.80, 3.60 and 5.40 J UVB. As shown in **Figure 3.8**, the decrease of UV-absorbance of all three polymers is a result of *trans* to *cis* photoisomerization of the cinnamate moiety in the polymer since the *cis* isomer has smaller ε value than the *trans* isomer. All three polymers are less photostable than the standard 2-ethylhexyl-*p*-methoxycinnamate (EHMC). It was speculated that this decrease in photostability was caused by the hydrophobic nature of poly(ethylene oxide) moieties in the oligomeric structures. Previous study on the *cis-trans* photoisomerization of EHMC [38], has indicated that the equilibrium between the two configurations depended

upon polarity of the solvent used. The equilibrium shifted to more *cis* isomer when polar solvent was used and *trans* to *cis* photoisomerization was more pronounced in more polar solvent.

trans-isomer
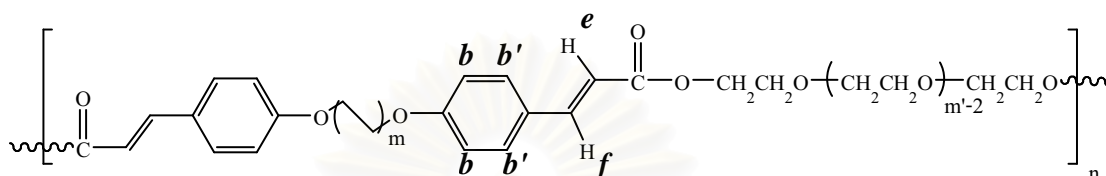
**cis-isomer**
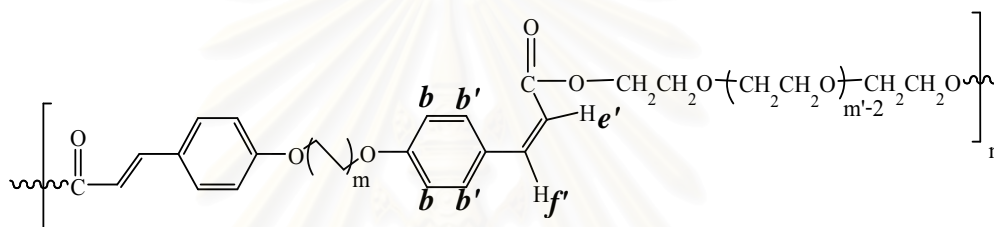
m = 1,6   m' = 4,9

P2-PEG200
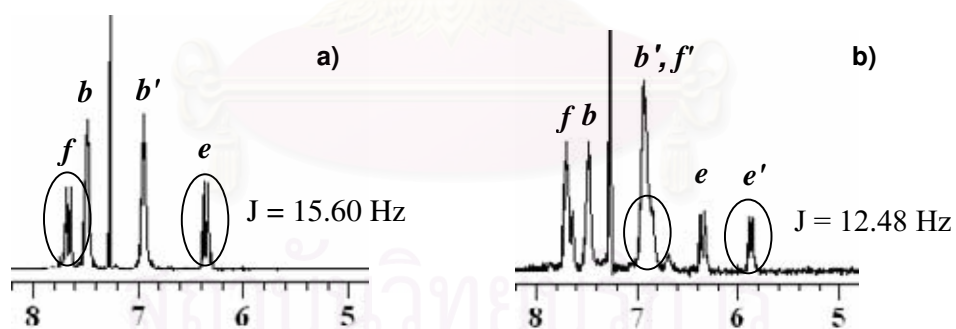
P2-PEG400
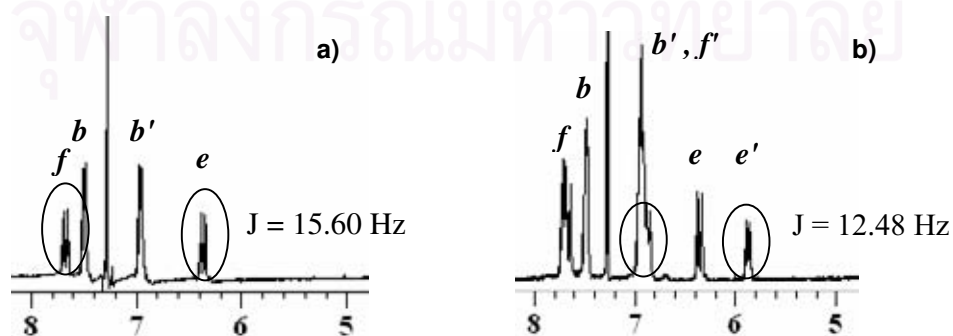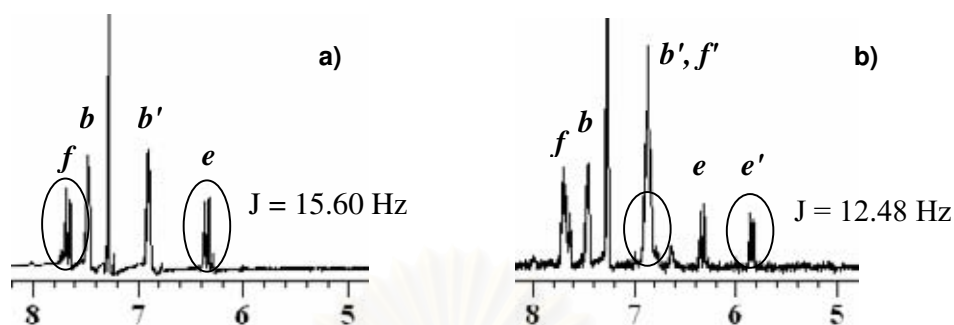
P12-PEG400

Figure 3.9 ^{1}H-NMR spectra of **P2-PEG200**, **P2-PEG400** and **P12-PEG400**; a) before UVA/UVB irradiation, b) after UVA/UVB irradiation. The irradiation was done for 6 hours at 3.0 mW/cm^{2} UVA and 0.25 mW/cm^{2} UVB

This was confirmed by ^{1}H-NMR spectra of the polymer before and after UV exposure. Obvious *trans* to *cis* isomerization could be seen from the two spectral pairs (**Figure 3.9**). The ^{1}H-NMR spectra of *trans*-cinnamates show two double signals at 7.68-7.63 (J=15.60 Hz, 1H, -Ar-C**H**=CH-COO-) and 6.38-6.32 ppm (J=15.60 Hz, 1H, -Ar-CH=C**H**-COO-). After UV exposure, the configurational change from *trans*- to *cis*-cinnamate was confirmed by the appearance of two double signals at 6.33-6.31 (J=12.48 Hz, 1H, -Ar-C**H**=CH-COO-) and 5.88-5.82 ppm (J=12.48 Hz, 1H, -Ar-CH=C**H**-COO-).

3.4 Syntheses of Nnano/microparticles

The obtained polymers are amphiphilic molecules with cinnamate moieties representing hydrophobic parts and polyethylene oxide moieties representing hydrophilic parts. Thus, preparation of the nano/microparticles from **P2-PEG400** and **P12-PEG400** were carried out by a solvent displacement technique. The obtained product is colloidal suspension. Particle size distribution analyzed by light scattering analysis (Zetasizer nanoseries) and by laser diffraction analysis (Mastersizer S), gave a size average of ~500 nm (**P2-PEG400**) and ~3 µm (**P12-PEG400**) (**Figure 3.10**). Transmittance electron micrograph of **P12-PEG400** (**Figure 3.10**) reveals semi-spherical shape.
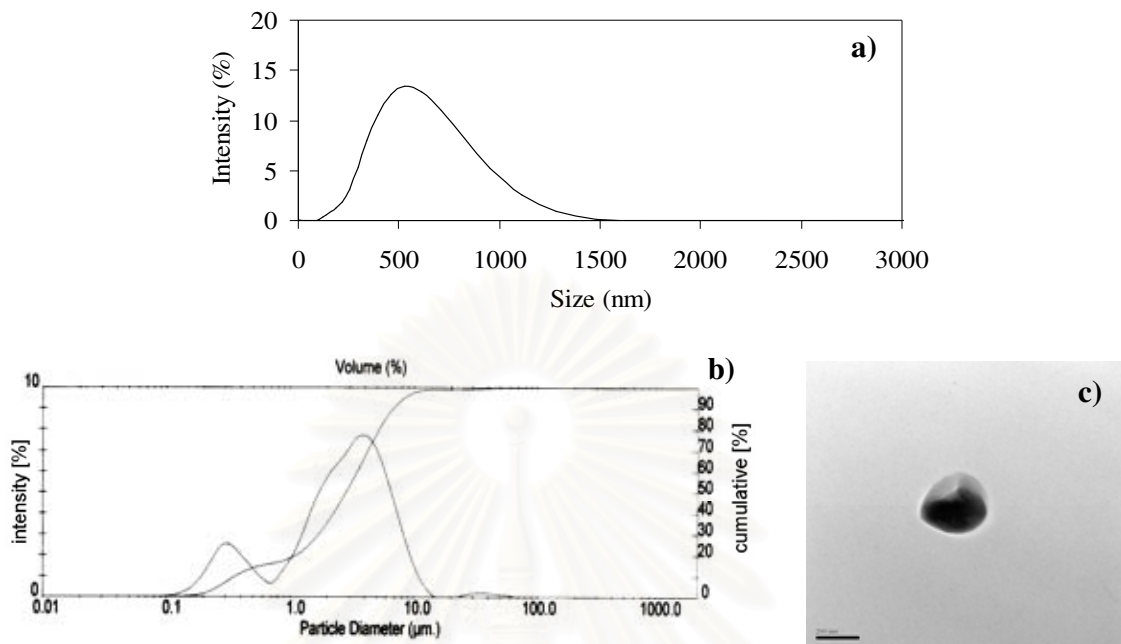
Figure 3.10 Size distributions of colloidal particles of **P2-PEG400** as obtained by laser diffraction analysis (Zetasizer nanoseries, Malvern Instruments Ltd.) (a), **P12-PEG400** as obtained by light scattering analysis (Mastersizer S, Malvern Instruments Ltd.) (b) and TEM image of the colloidal particles of **P12-PEG400** (c)

CHAPTER IV
CONCLUSION

In this work, poly((1,2-(bis(4-(2-carboxyvinyl)phenoxy))ethane)-*co*-(poly (ethylene glycol)200)), poly((1,2-(bis(4-(2-carboxyvinyl)phenoxy))ethane)-*co*-(poly (ethylene glycol)400)) and poly((1,12-(bis(4-(2-carboxyvinyl)phenoxy))dodecane)-*co*-(poly(ethylene glycol)400)) were synthesized. Syntheses of these three UV screening polyesters were accomplished by esterification between the synthesized monomers (dicinnamic acid) with poly(ethylene glycol) through the acid chloride method.

m = 1,6   m' = 4,9
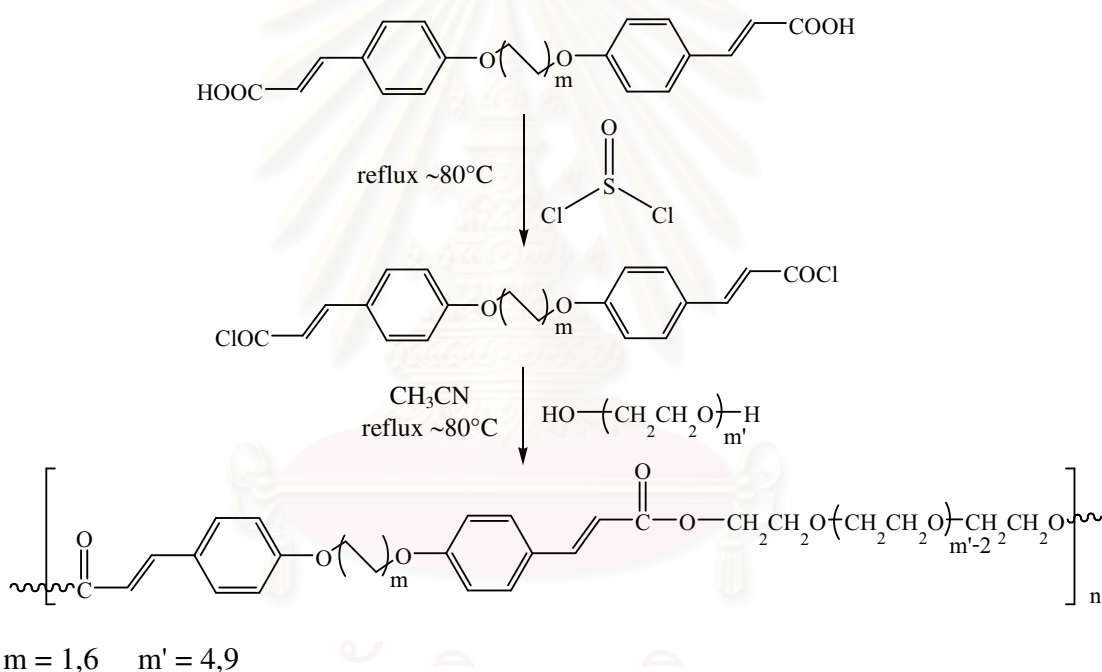
UV absorption properties of each polyesters indicate UVB screening properties. However all three polyester were less photostable than the standard 2-ethylhexyl-*p*-methoxycinnamate (EHMC). This less photostability is probably caused by a nature of poly(ethylene oxide) chain.

P2-PEG400 is yellow liquid, miscible with various organic solvents. Its liquid nature makes applications in cosmetic formulations possible.

In addition, a yellow oil **P2-PEG400** and a yellow wax **P12-PEG400** can be processed into nano/microparticles of average particle size of 500 nm and 3 μm, respectively. This UV screening particles may be further developed into cosmetic carrier with UV filtering property.

REFERENCES

[1] Laethem, A. V.; Claerhout, S.; Garmyn, M.; and Agostinis, P. The sun burn cell: Regulation of death and survival of the keratinocyte. *The International Journal of Biochemistry & cell biology* 37 (2005): 1547-1553.

[2] Halliday, G. M. Inflammation, gene mutation and photoimmunosuppression in response to UVA-induced oxidative damage. *Mutation Research* 571 (2005): 107-120.

[3] Cadet, J.; Sage, E.; and Douki, T. Ultraviolet radiation-mediated damage to cellular DNA. *Mutation Research* 571 (2005): 3-17.

[4] Pfeifer, G. P.; You, Y. H.; and Besaratinia, A. Mutations induced by ultraviolet light. *Mutation Research* 571 (2005): 19-31.

[5] Krutmann, J. Ultraviolet A radiation-induced biological effects in human skin: relevance for photoaging and photodermatosis. *Journal of Dermatological Science* 23 (2001): S22-S26.

[6] Courdavault, S.; Baudouin, C.; Charveron, M.; Favier, A.; Cadet, J.; and Douki, T. Larger yield of cyclobutane dimers than 8-oxo-7,8-dihydroguanine in the DNA of UVA-irradiated human skin cells. *Mutation Research* 556 (2004): 135-142.

[7] Courdavault, S.; Baudouin, C.; Charveron, M.; Canguilhem, B.; Favier, A.; Cadet, J.; and Douki, T. Repair of the three main types of bipyrimidine DNA photoproducts in human keratinocytes exposed to UVB and UVA radiations. *DNA Repair* 4 (2005): 836-844.

[8] Draelos, Z. D.; Dover, J. S.; and Alam, M. *Cosmeceuticals.* Philadelphia: Elsevier Saunders, 2005, pp 139-147.

[9] Ricci, C.; Pazzaglia, M.; and Tosti, A. Photocontact dermatitis from UV filters. *Contact Dermatitis* 38 (1998): 343-344.

[10] Darvay, A.; White, I. R.; Rycroft, R. J. G.; Jonnes, A. B.; Hawk, J. L.; and McFadden, J. P. Photoallergic contact dermatitis is uncommon. *British Journal of Dermatology* 145 (2001): 597-601.

[11] Mitchell, K.; and Mitchnick, M. Visibly transparent UV sunblock agents and methods of making same. US Patent No. 5587148 (1996).

[12] Serpone, N.; Dondi, D.; and Albino, A. Inorganic and organic UV filters: Their role and efficacy in sunscreens and suncare products. *Inorganic Chimica Acta* 360 (2007): 794-802.

[13] Kertesz, Z.; Szikszai, Z.; Gontier, E.; Moretto, P.; Surleve-Bazeille, J. E.; Kiss, B.; Juhasz, I.; Hunyadi, J.; and Kiss, A. Z. Nuclear microprobe study of TiO$_2$-penetration in the epidermis of human skin xenografts. *Nuclear Instruments and Methods in Physicals Research B* 231 (2005): 280-285.

[14] Gamer, A. O.; Leibold, E.; and Ravenzwaay, B. The in vitro absorption of microfine zinc oxide and titanium dioxide through porcine skin. *Toxicology in Vitro* 20 (2006): 301-307.

[15] Villalobos-Hernandez, J. R.; and Muller-Goymann, C. C. Sun protection enhancement of titanium dioxide crystals by the use of carnauba wax nanoparticles: The synergistic interaction between organic and inorganic sunscreens at nonoscale. *International Journal of Pharmaceutics* 322 (2006): 161-170.

[16] Hanny, J.; and Nagel, R. Detection of sunscreen agents in human breast milk. *Deutsche Lebensmittel-Rundschau* 91 (1995): 341-345.

[17] Hagedorn-Leweke, U.; and Lippole, B. C. Absorption of sunscreens and other compounds through human skin *in vivo*: Derivation of a method to predict maximum fluxes. *Pharmaceutical Research* 12 (1995): 1354-1360.

[18] Hyden, C. G. J.; Roberts, M. S.; and Benson, A. E. Systemic absorption of sunscreen after topical application. *Lancet* 350 (1997): 863-864.

[19] Gupta, V. K.; Zatz, J. L.; Rerek, M. Percutaneous absorption of sunscreens though micro-Yucatan pig skin *in vitro*. *Pharmaceutical Research* 16 (1999): 1602-1607.

[20] Potard, G.; Laugel, C.; Baillet, A.; Schaefer, H.; and Marty, J. P. Quantitative HPLC analysis of sunscreens and caffeine during in vitro percutaneous penetration studies. *International Journal Pharmaceutics* 189 (1999): 249-260.

[21] Potard, G.; Laugel, C.; Schaefer, H.; and Marty, J. P. The stripping technique: In vitro absorption of five UV filters on excised fresh human skin. *Skin Pharmacology and Applied Skin Physiology* 13 (2000): 336-344.

[22] Sarveiya, V.; Risk, S.; and Benson, H. A. E. Liquid chromatographic assay for common sunscreen agents: application to in vitro assessment of skin penetration and systemic absorption in human volunteers. *Journal Chromatography B* 803 (2004): 225-231.

[23] Carpenter, T.; Howe, A.; O'Connor, A.; Orfanelli, J.; and Siegfried, R. Protection from sun protectors. *Drug & Cosmetic Industry* 158 (1996): 56-103.

[24] Hossel, P.; Wunsch, T.; and Dieing, R. Cosmetic or dermatological sunscreen preparations. US Patent 2001/0021375A1 (2001).

[25] Godwin, D. A.; Kim, N. H.; and Felton, L. A. Influence of Transcutol$^{®}$ CG on the skin accumulation and transdermal permeation of ultraviolet absorbers. *European Journal of Pharmaceutics and Biopharmaceutics* 53 (2002): 23-27.

[26] Yener, G.; Incegul, T.; and Yener, N. Importance of using solid lipid microspheres as carriers for UV filters on the example octyl methoxy cinnamate. *International Journal of Pharmaceutics* 258 (2003): 203-207.

[27] Jimenez, M. M.; Pelletier, J.: Bobin, M. F.; and Martini, M. C. Influence of encapsulation on the in vitro percutaneous absorption of octyl methoxycinnamate. *International Journal of Pharmaceutics* 272 (2004): 45-55.

[28] Pattanaargson, S.; Hongchinnagorn, N.; Hirunsupachot, P.; and Sritana-anant, Y. UV absorption and photoisomerization of *p*-methoxycinnamate grafted silicone. *Photochemistry and Photobiology* 80 (2004): 322-325.

[29] Olvera-Martinez, B. I.; Cazares-Delgadillo, J.; Calderilla-Fajardo, S. B.; Villalobos-Garcia, R.; Ganem-Quintanar, A.; and Quintanar-Guerrero, D. Preparation of polymeric nanocapsules containing octyl methoxycinnamate by the Emulsification-Diffusion Thechnique: Penetration across the stratum corneum. *Journal of Pharmaceutical Sciences* 94 (2005): 1552-1559.

[30] Langer, M. E.; and Khorshahi, F. High loading water-dispersible UVA and/or UVB light-absorbing copolymer. US Patent No. 5250652 (1993).

[31] Richard, H.; and Ledue, M. Silicone-substituted cinnamide/malonamide/malonate compounds and photoprotective compositions comprised thereof. US Patent No. 6080880 (2000).

[32] O'Lenick, A. J. Aromatic dimethicone copolyol polymers as sunscreen agents. US Patent No. 6346595B1 (2002).

[33] Ledue, M.; Richard, H.; and Lagrange, A. Photoprotective/cosmetic compositions comprising novel benz-x-azole-substituted silane/siloxane sunscreens. US Patent No. 6376679B2 (2002).

[34] Koshti, N. M.; and Naik, S. D. Salt and heat sensitive, substantive UV-absorbing polymers. US Patent No. 7087692B2 (2006).

[35] Saminathan, M.; and Pillai, C. K. S. Synthesis of novel liquid crystalline polymers with cross-linked network structures. *Polymer* 41 (2000): 3103-3108.

[36] Jo, S.; Engel, P. S.; and Mikos, A. G. Synthesis of poly(ethylene glycol)-tethered poly(propylene fumarate) and its modification with GRGD peptide. *Polymer* 41 (2000): 7595-7604.

[37] Behniafar, H.; Akhlaghinia, B.; and Habibian, S. Synthesis and characterization of new soluble and thermally stable poly(ester-imide)s derived from N-[3,5-bis(N-trimellitoyl)phenyl]phthalimide and various bisphenols. *European Polymer Journal* 41 (2005): 1071-1078.

[38] Pattanaargson, S.; Munhapol, T.; Hirunsupachot, P.; and Luangthongaram, P. Photoisomerization of octyl methoxycinnamate. *Journal of Photochemistry and Photobiology A: Chemistry* 161 (2004): 269-274.

APPENDICES

APPENDIX A

A.1 Calculation of molar absorptivity of monomer/polymer

$$\text{x ppm} \quad = \quad \frac{x \times 10^{-3}}{\text{Molecular weight}} \quad \text{moles of monomer/1000 mL}$$

$$= \quad \frac{x \times 10^{-3}}{\text{Molecular weight (polymeric unit)}} \quad \text{moles of polymer/1000 mL}$$

By plotting a graph between absorbance (at λ_{max}) and concentrations (x) of each monomer/polymer sample, a linear relationship was obtained with its slope represented the molar absorptivity (ε) of the monomer/polymer.
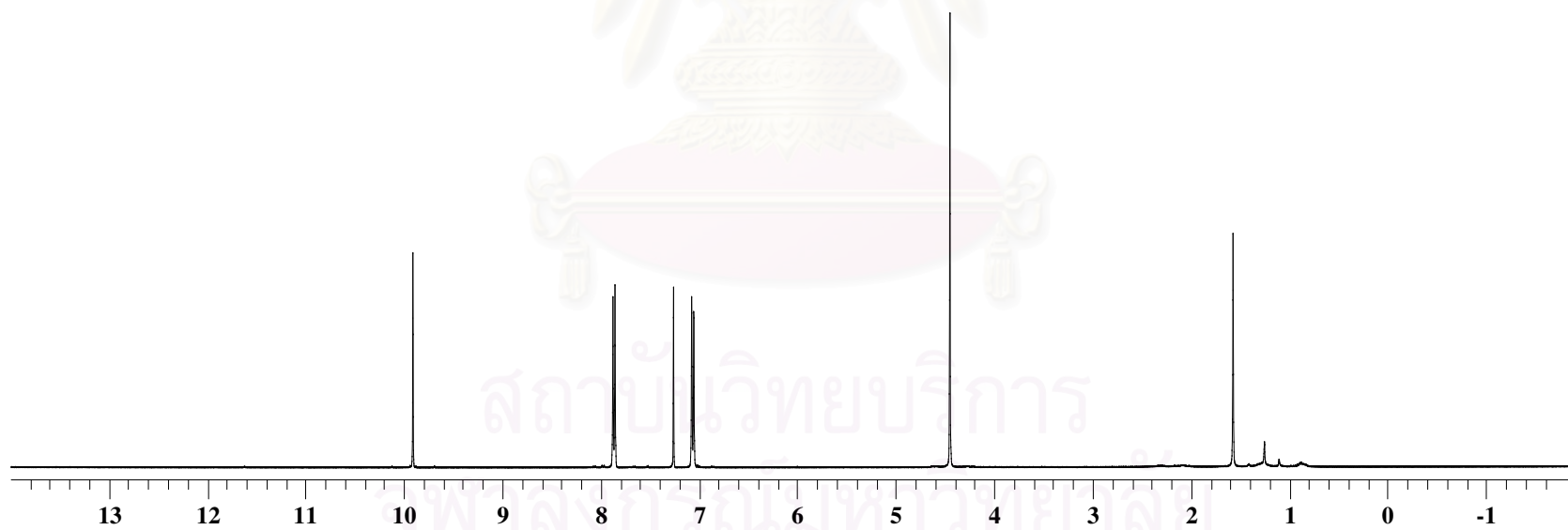
Figure B.1 ^{1}H-NMR (CDCl$_3$) spectrum of 1,2-(bis(4-(formylphenoxy))ethane), (**mm2**)
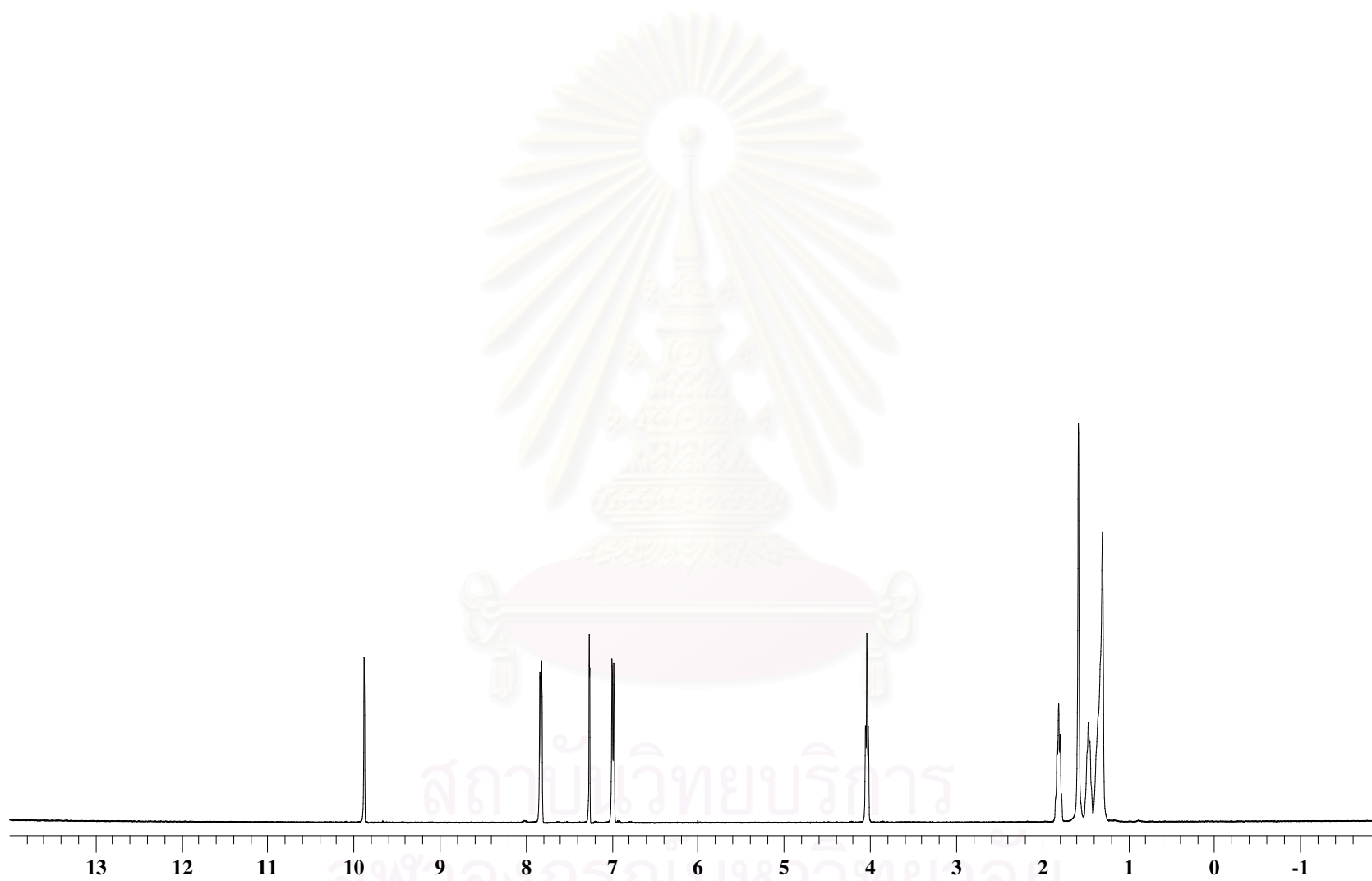
Figure B.2 ^{1}H-NMR (CDCl$_3$) spectrum of 1,12-(bis(4-(formylphenoxy))dodecane), (**mm12**)
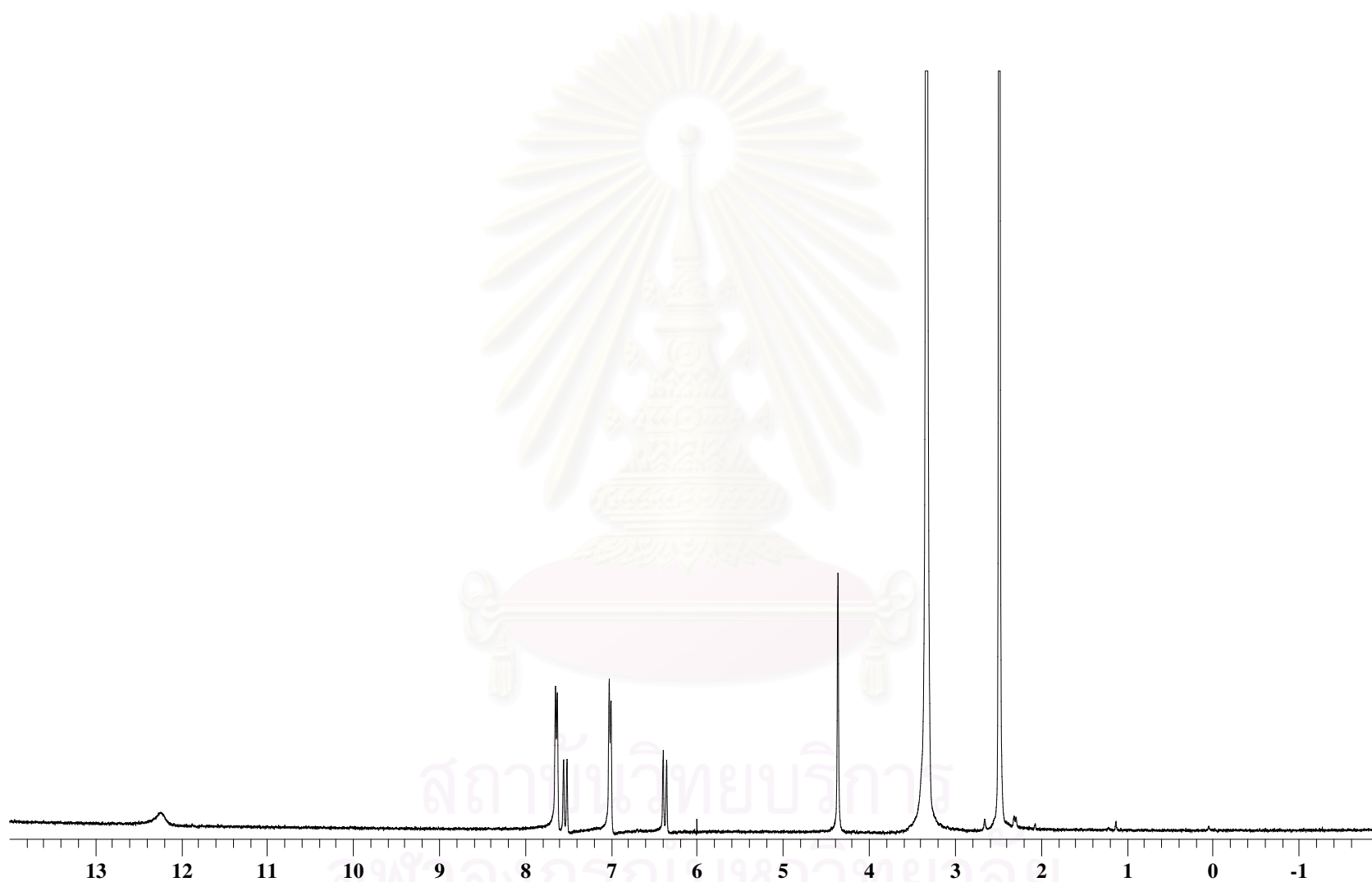
Figure B.3 ^{1}H-NMR (DMSO-d_6) spectrum of 1,2-(bis(4-(2-carboxyvinyl)phenoxy))ethane, (**M2**)
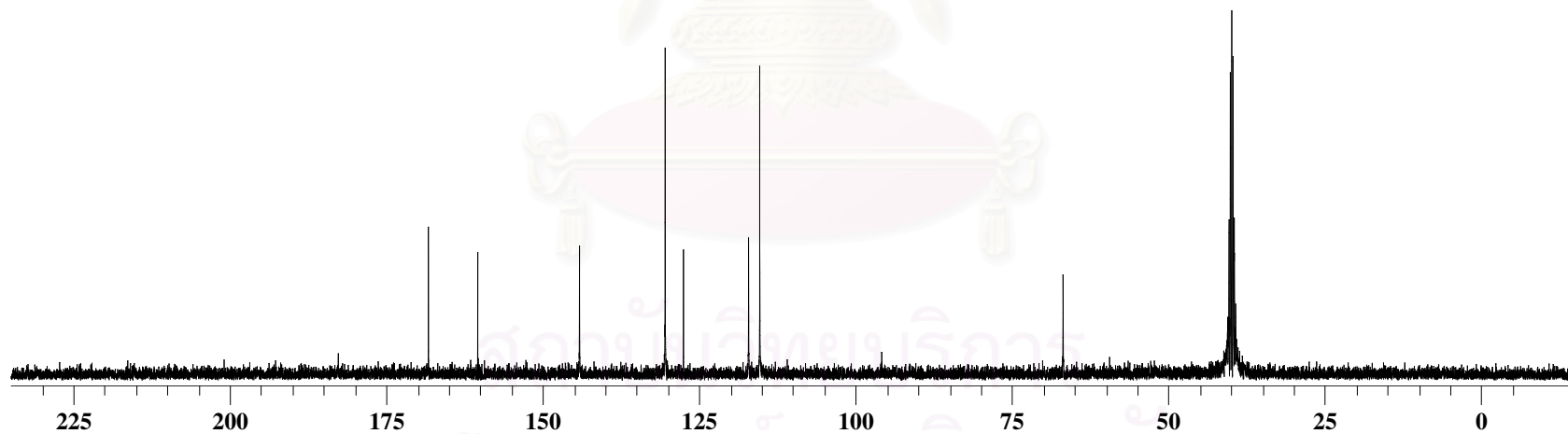
Figure B.4 ^{13}C-NMR (DMSO-d_6) spectrum of 1,2-(bis(4-(2-carboxyvinyl)phenoxy))ethane, (**M2**)
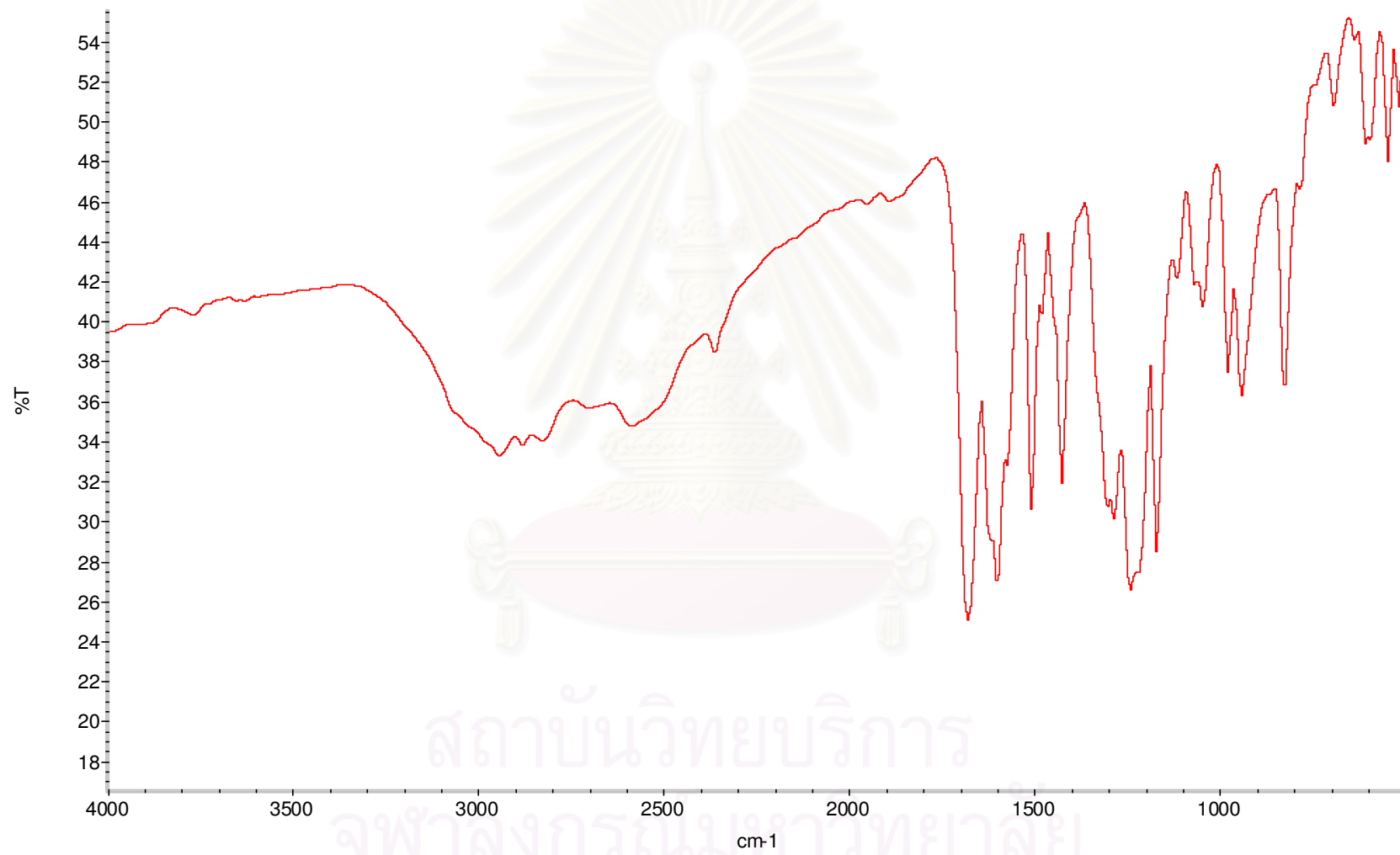
Figure B.5 FT-IR spectrum of 1,2-(bis(4-(2-carboxyvinyl)phenoxy))ethane, (**M2**)
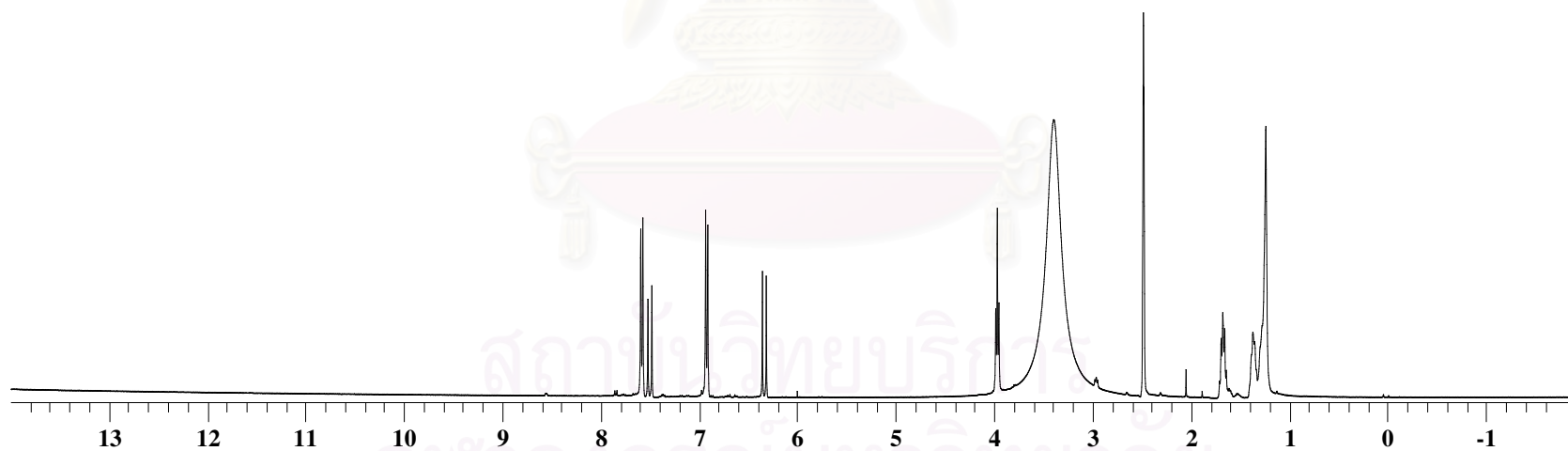
Figure B.6 ^{1}H-NMR (DMSO-d_6) spectrum of 1,12-(bis(4-(2-carboxyvinyl)phenoxy))dodecane, (**M12**)
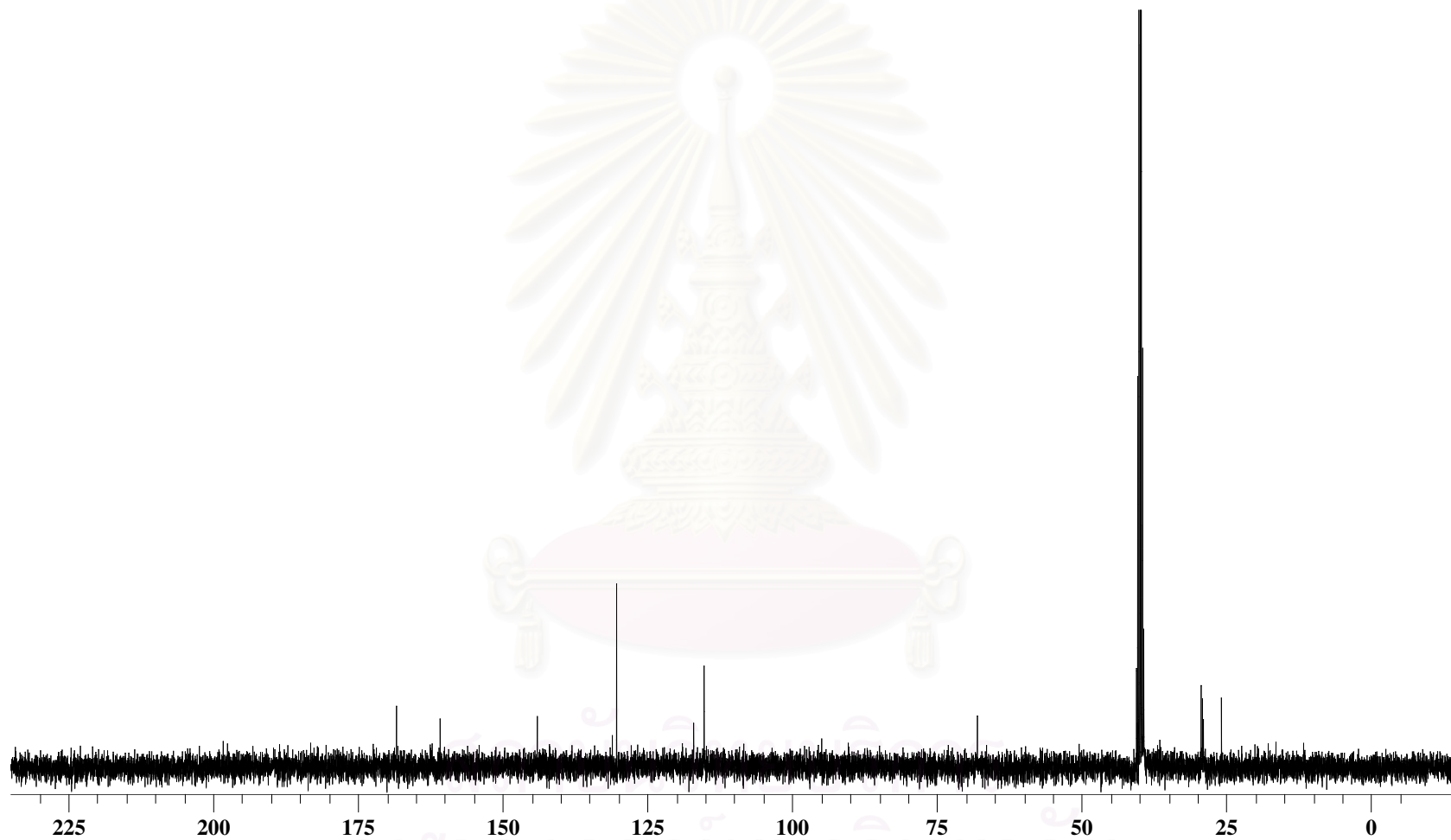
Figure B.7 ^{13}C-NMR (DMSO-d_6) spectrum of 1,12-(bis(4-(2-carboxyvinyl)phenoxy))dodecane, (**M12**)
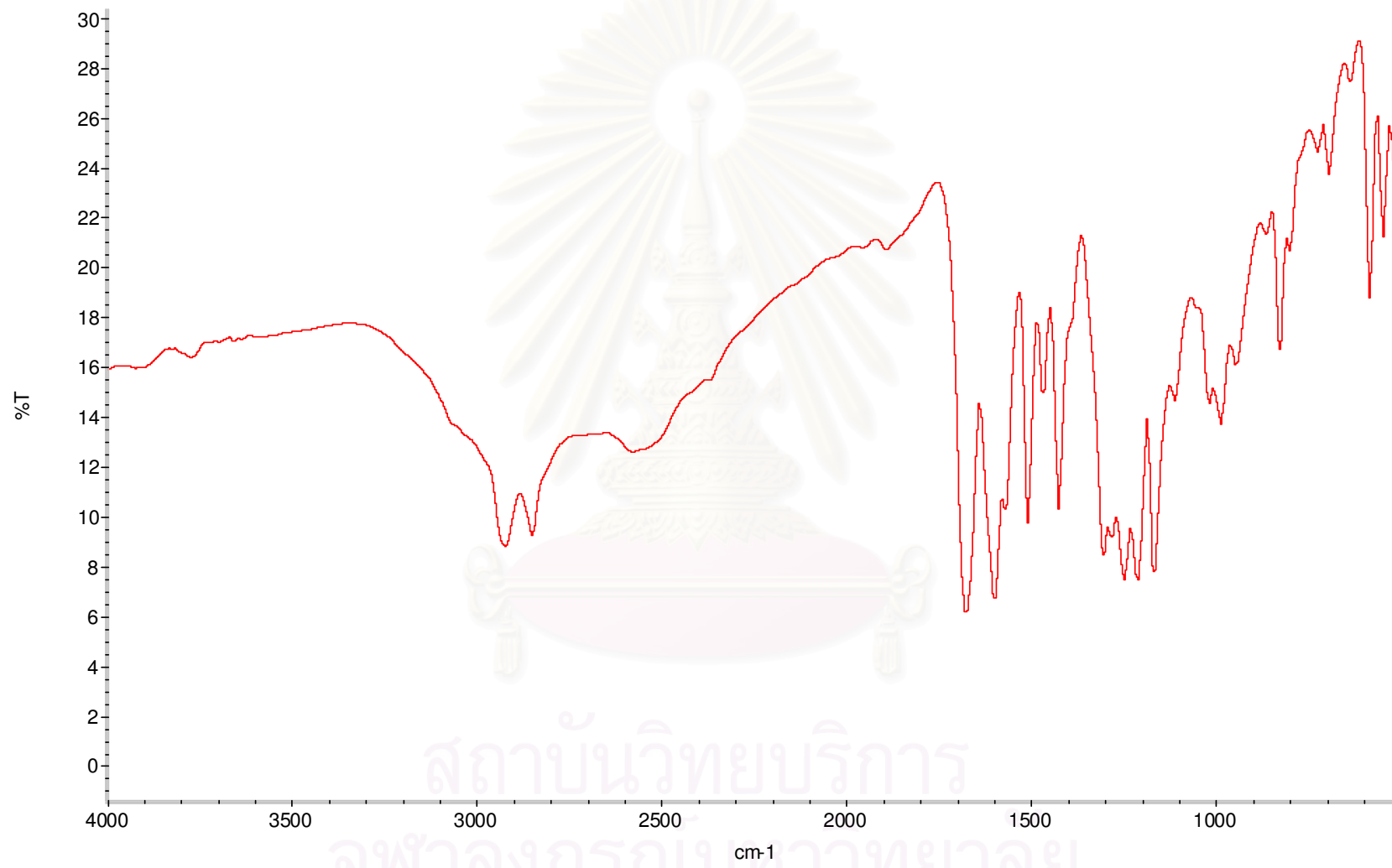
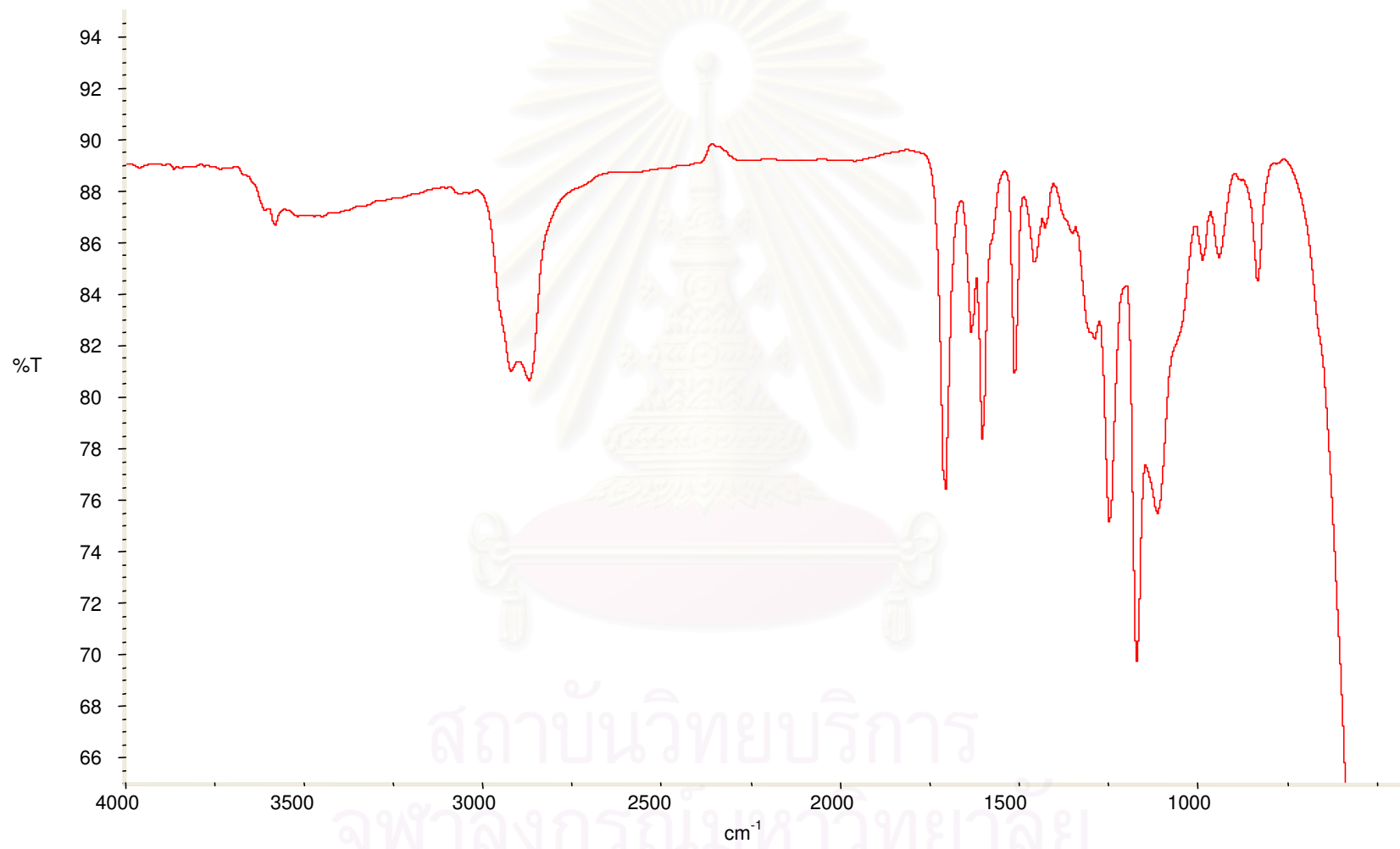**Figure B.8** FT-IR spectrum of 1,12-(bis(4-(2-carboxyvinyl)phenoxy))dodecane, (**M12**)
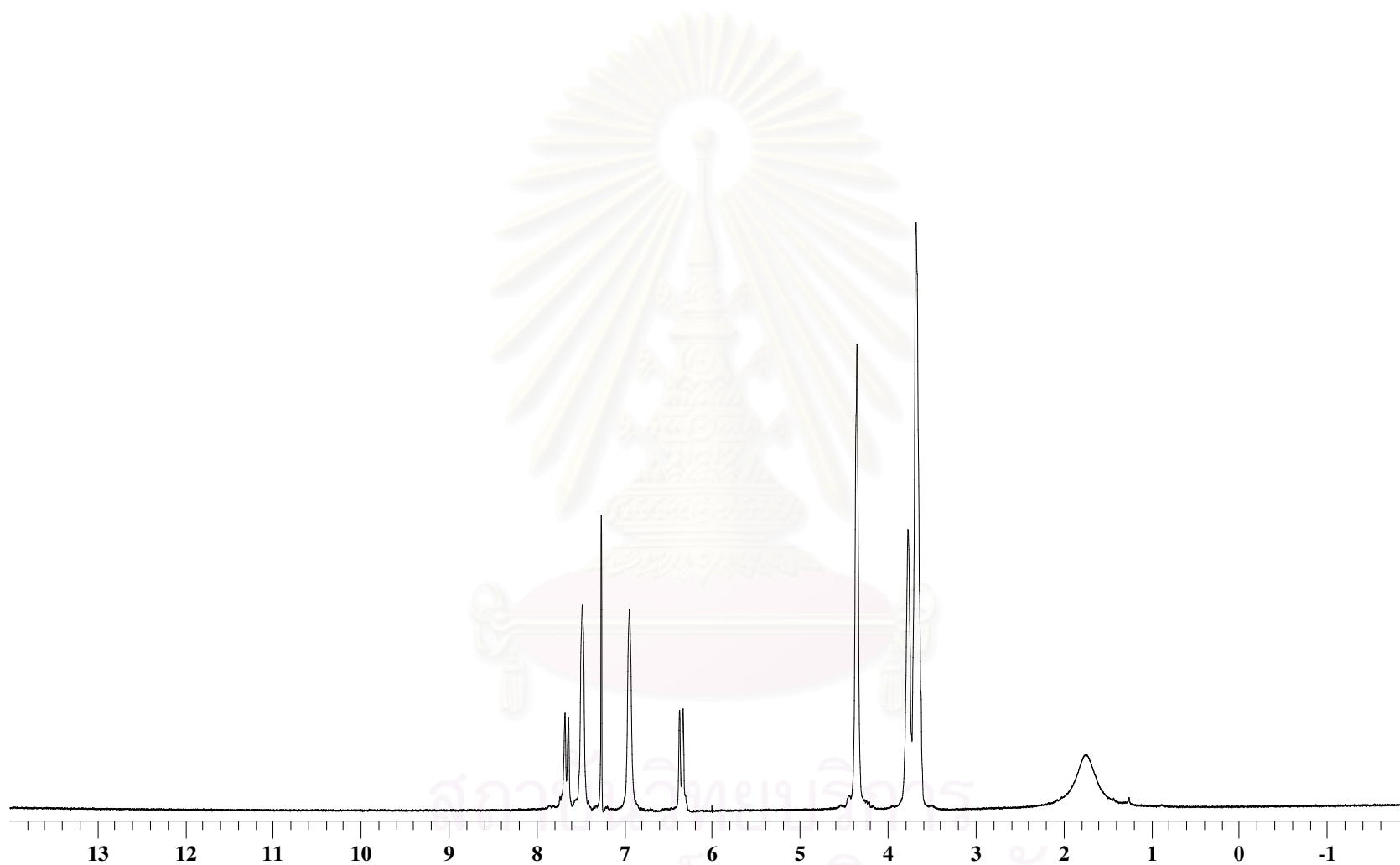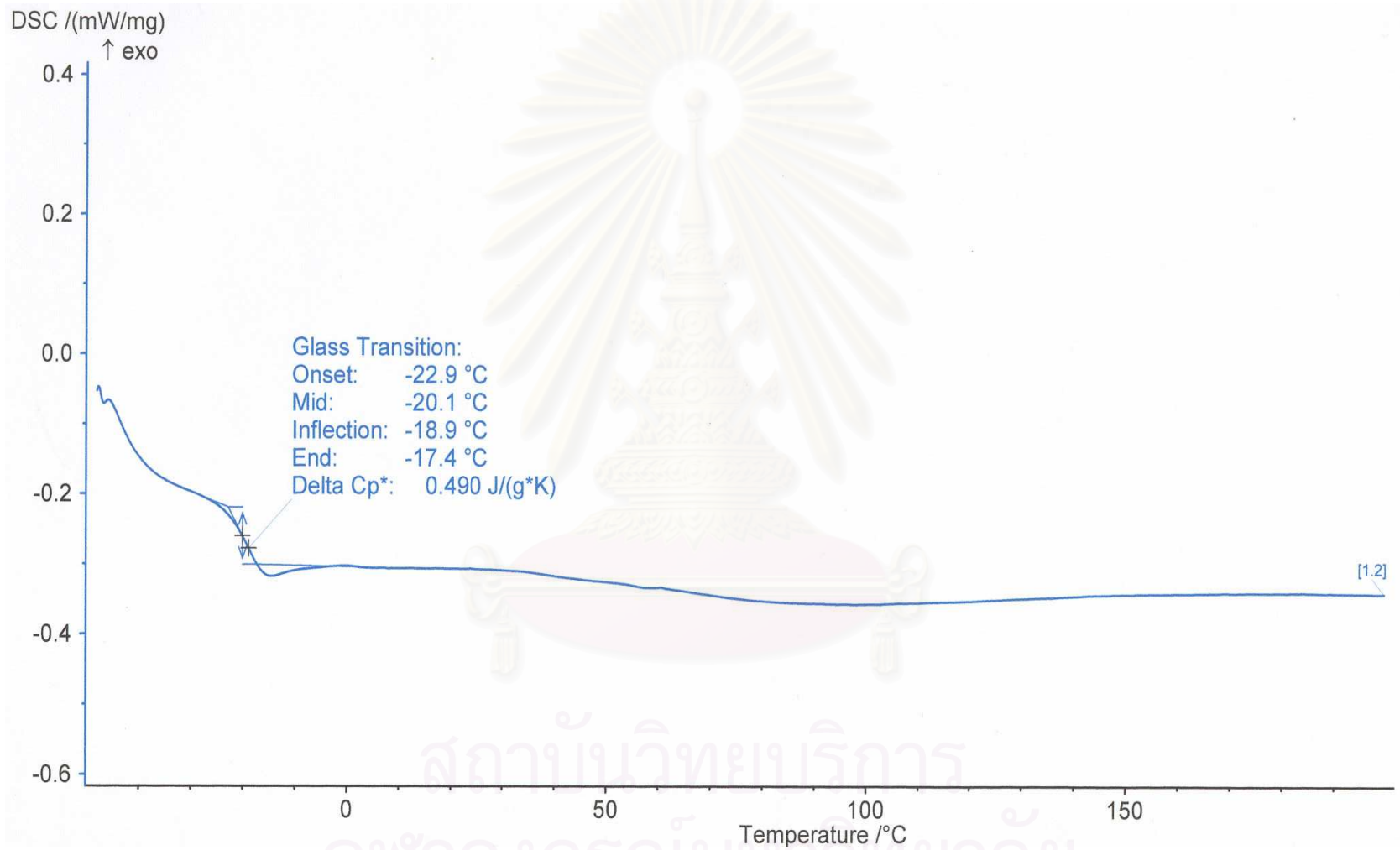
Figure B.9 ^{1}H-NMR (CDCl$_3$) spectrum of poly((1,2-(bis(4-2-carboxyvinyl)phenoxy))ethane)-*co*-(poly(ethylene glycol)200)),
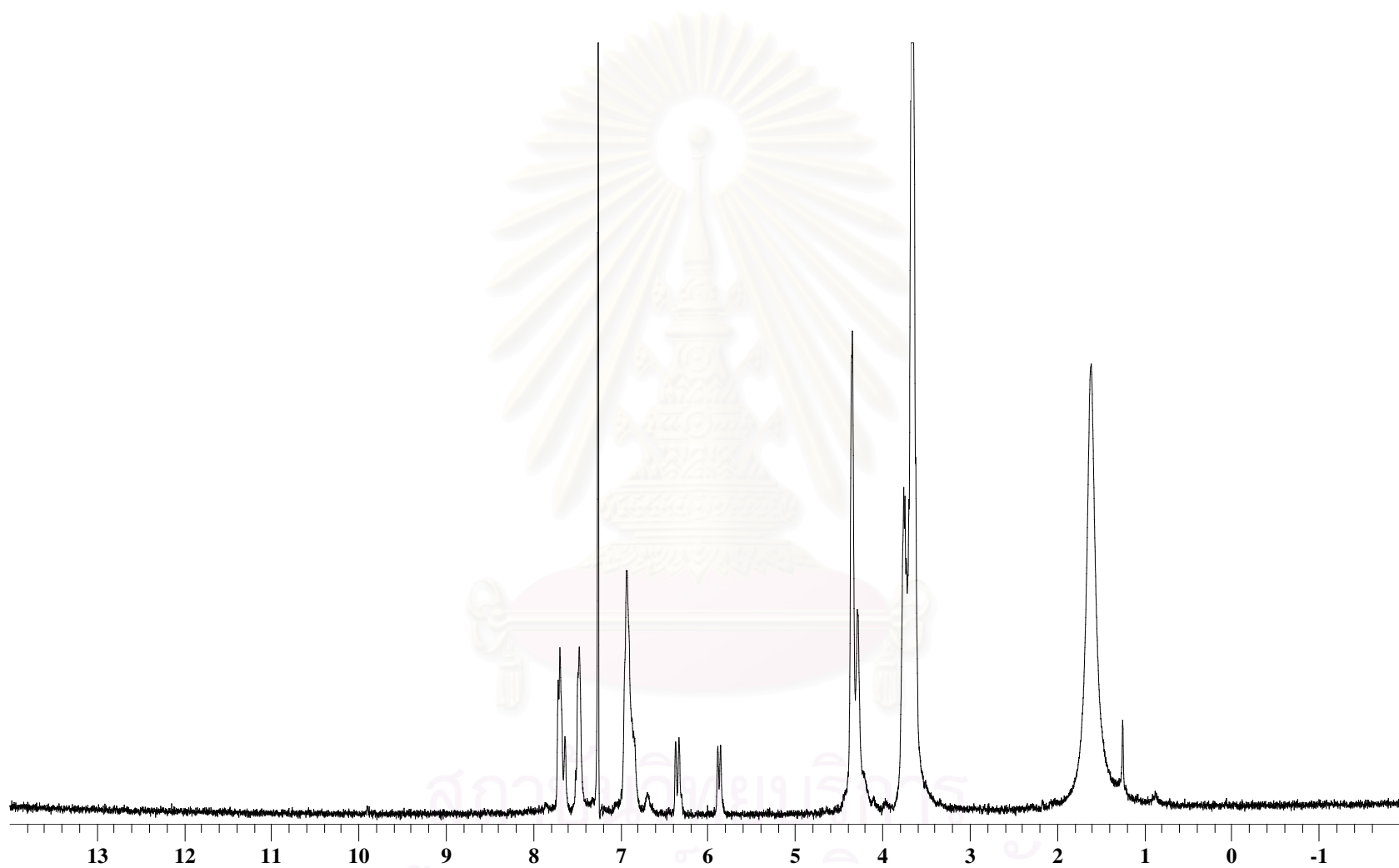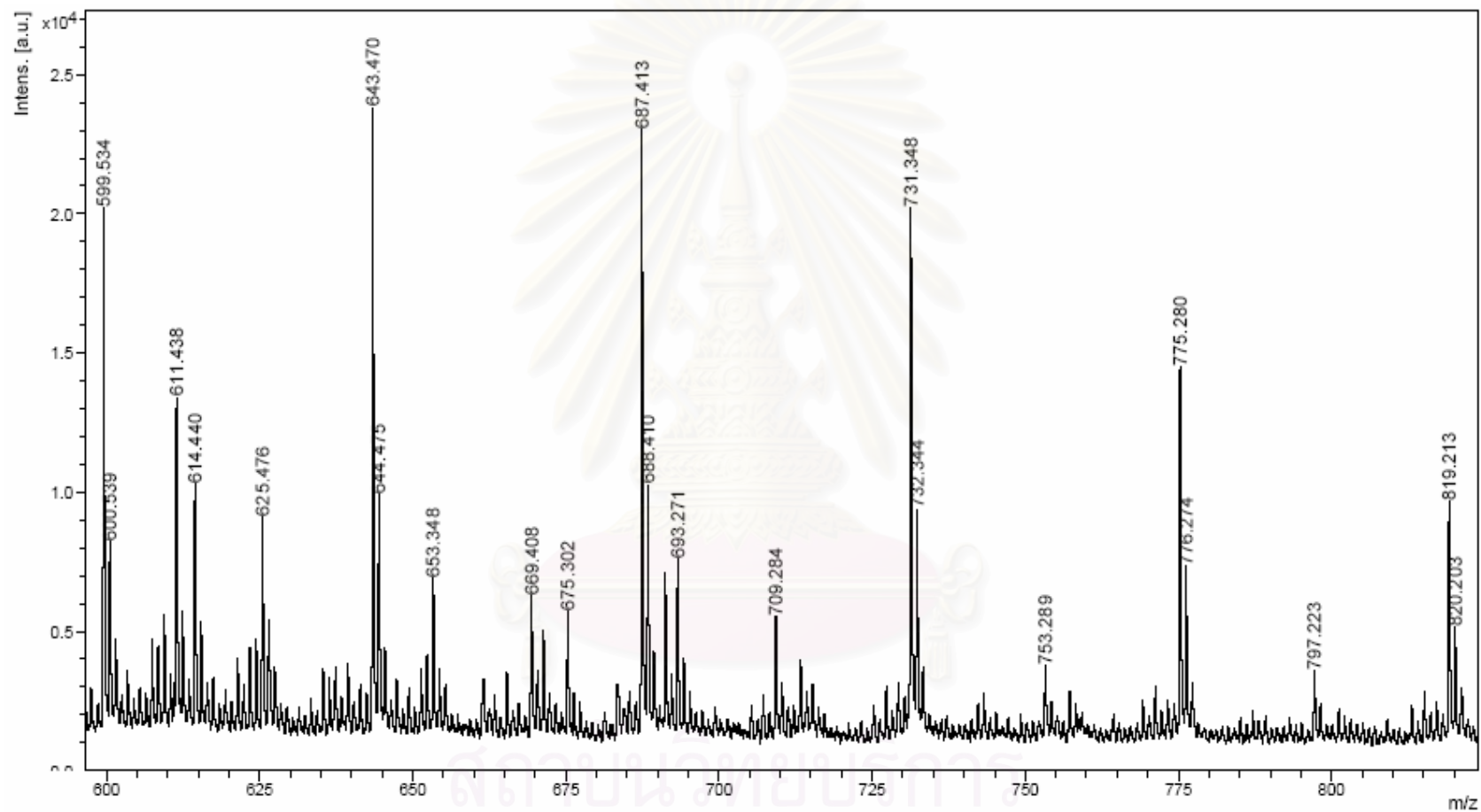
P2-PEG200

Figure B.10 ¹H-NMR (CDCl₃) spectrum of poly((1,2-(bis(4-2-carboxyvinyl)phenoxy))ethane)-*co*-(poly(ethylene glycol)200)), **P2-PEG200** irradiated
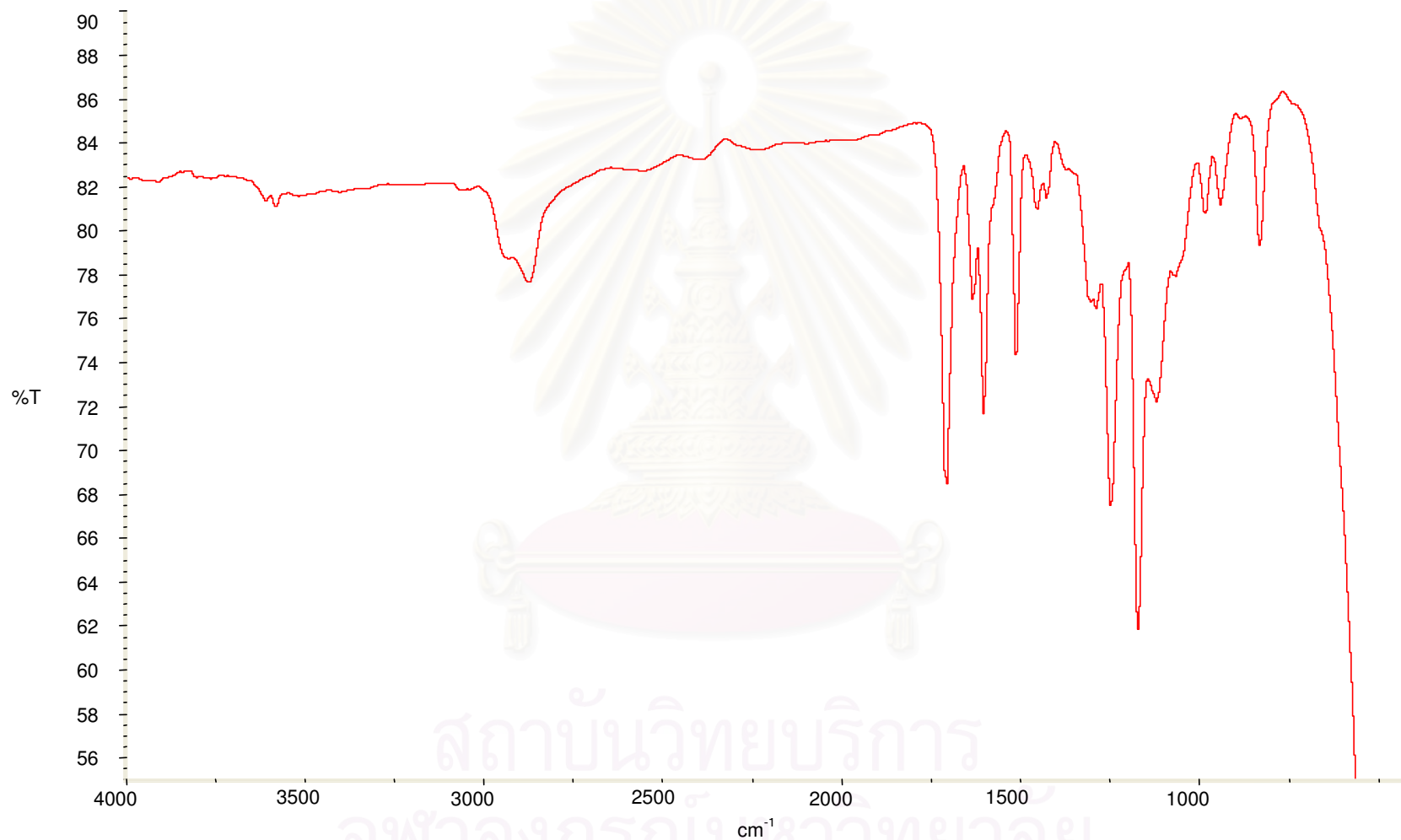
Figure B.11 FT-IR spectrum of poly((1,2-(bis(4-2-carboxyvinyl)phenoxy))ethane)-*co*-(poly(ethylene glycol)200)), **P2-PEG200**
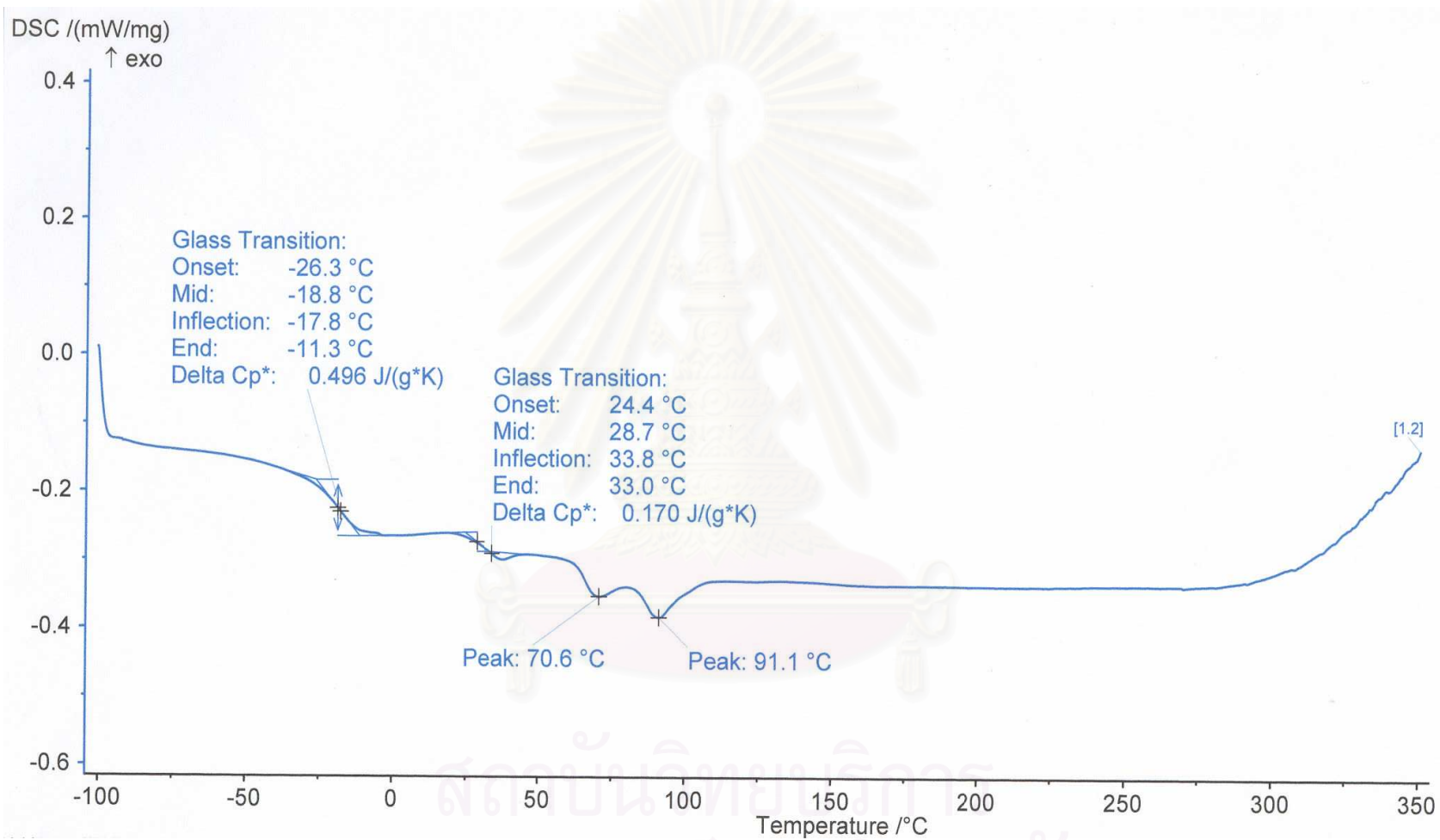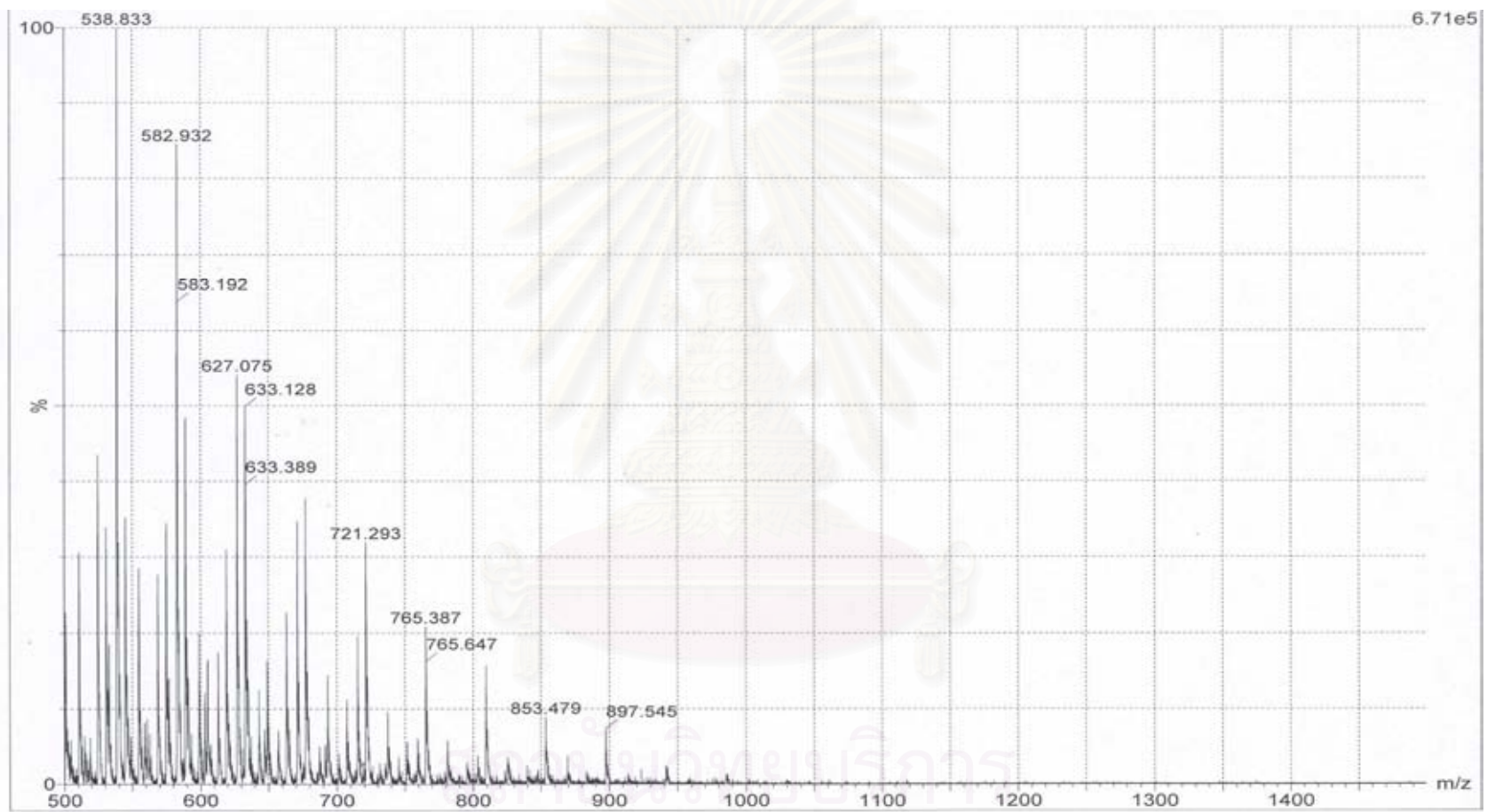
Figure B.12 DSC spectrum of poly((1,2-(bis(4-2-carboxyvinyl)phenoxy))ethane)-*co*-(poly(ethylene glycol)200)), **P2-PEG200**
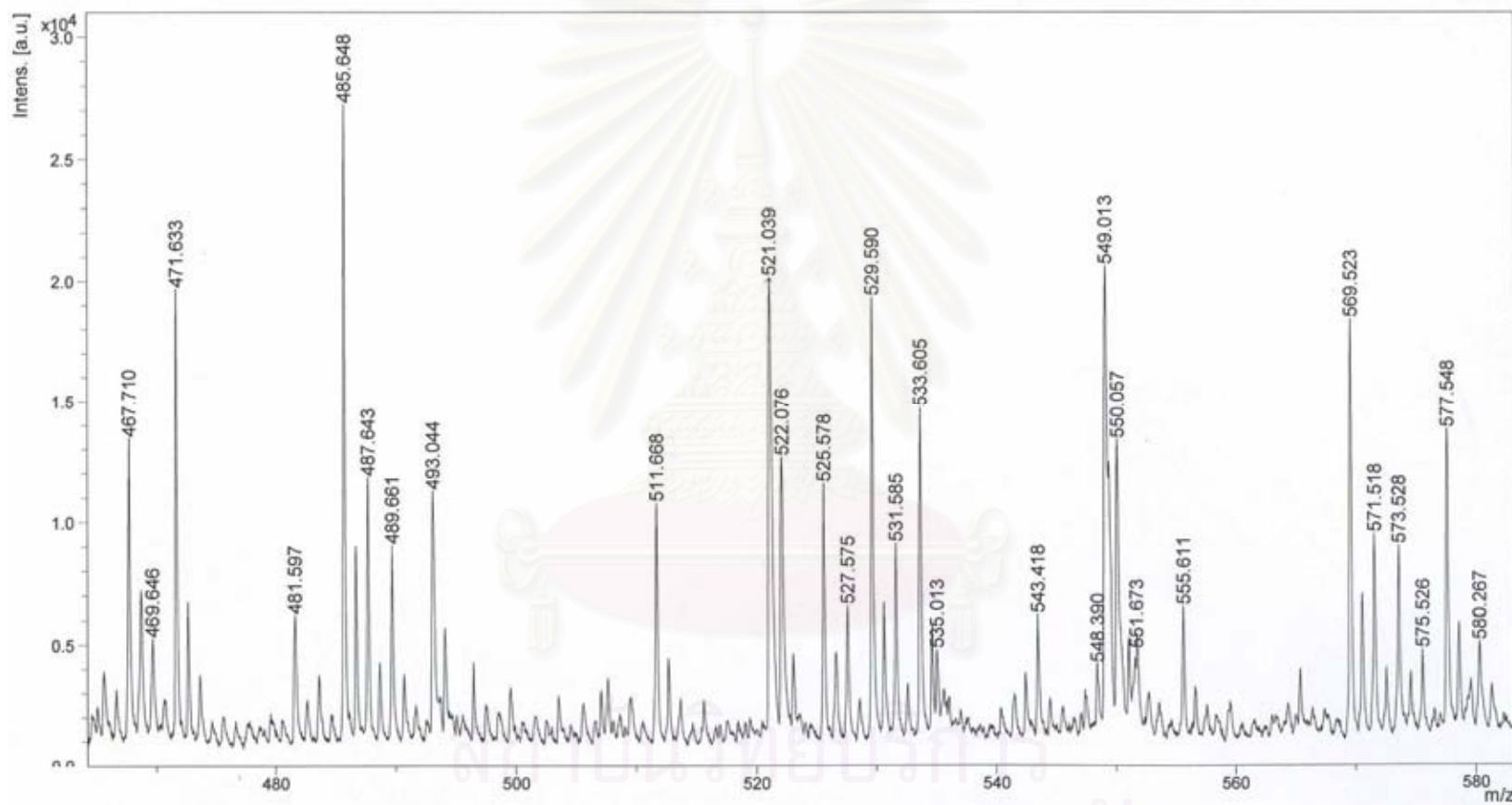
Figure B.13 Mass spectrum of poly((1,2-(bis(4-2-carboxyvinyl)phenoxy))ethane)-*co*-(poly(ethylene glycol)200)), **P2-PEG200**

[MULDI-TOF MS]
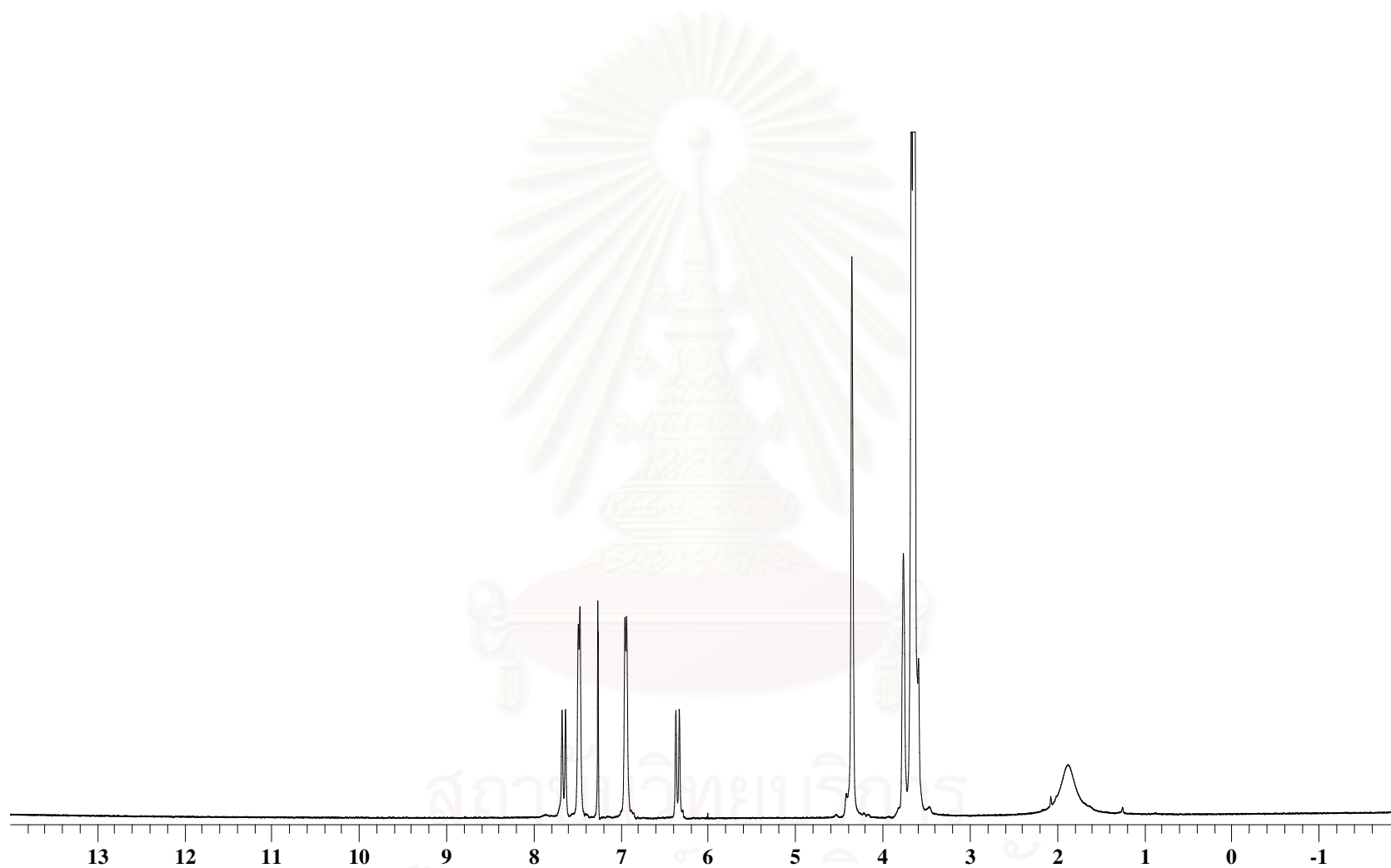
Figure B.14 ^{1}H-NMR (CDCl$_3$) spectrum of poly((1,2-(bis(4-2-carboxyvinyl)phenoxy))ethane)-*co*-(poly(ethylene glycol)400)), **P2-PEG400**
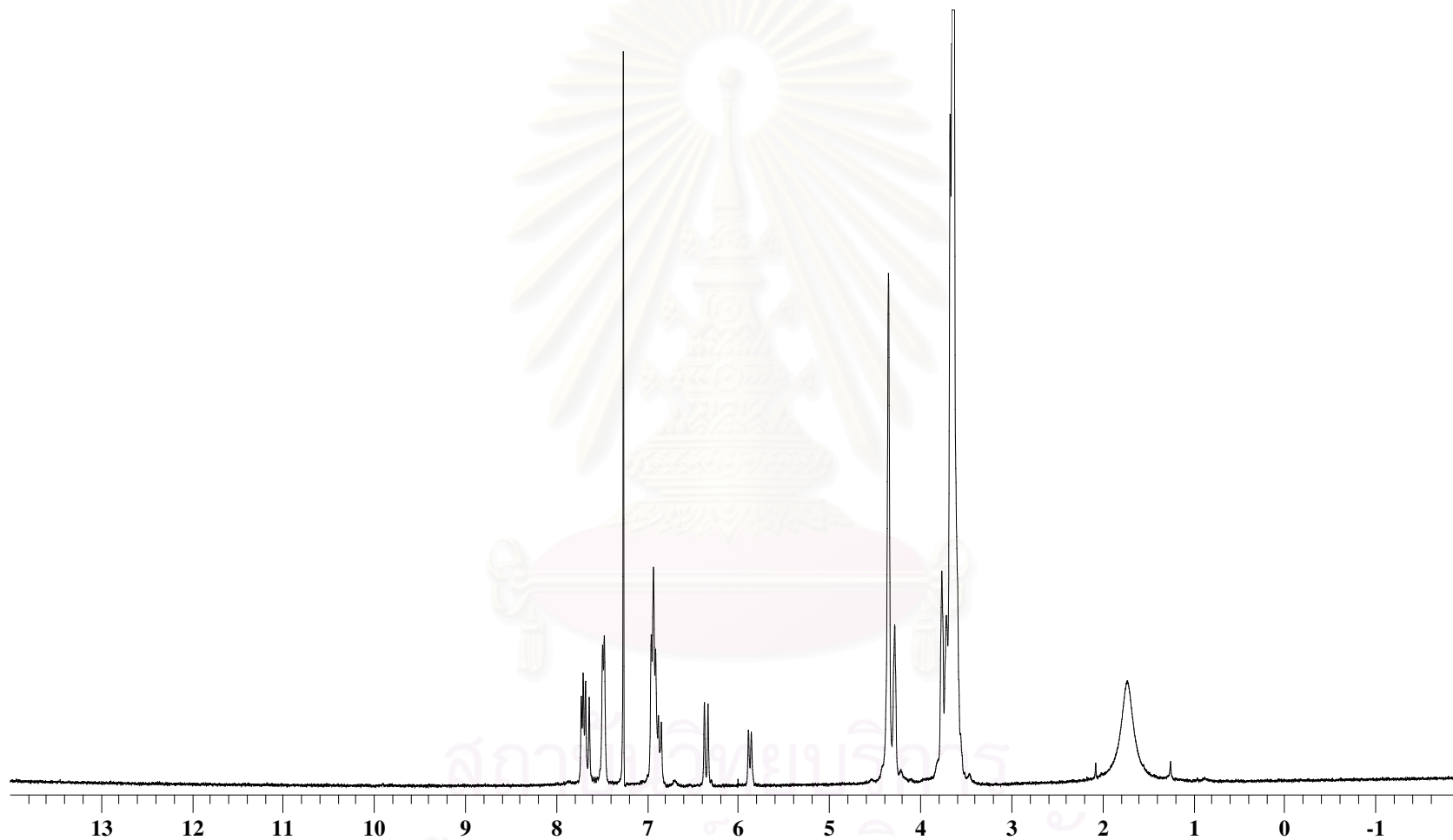
Figure B.15 ^{1}H-NMR (CDCl$_3$) spectrum of poly((1,2-(bis(4-2-carboxyvinyl)phenoxy))ethane)-*co*-(poly(ethylene glycol)400)), **P2-PEG400** irradiated

Figure B.16 FT-IR spectrum of poly((1,2-(bis(4-2-carboxyvinyl)phenoxy))ethane)-*co*-(poly(ethylene glycol)400)), **P2-PEG400**

Figure B.17 DSC spectrum of poly((1,2-(bis(4-2-carboxyvinyl)phenoxy))ethane)-*co*-(poly(ethylene glycol)400)), **P2-PEG400**
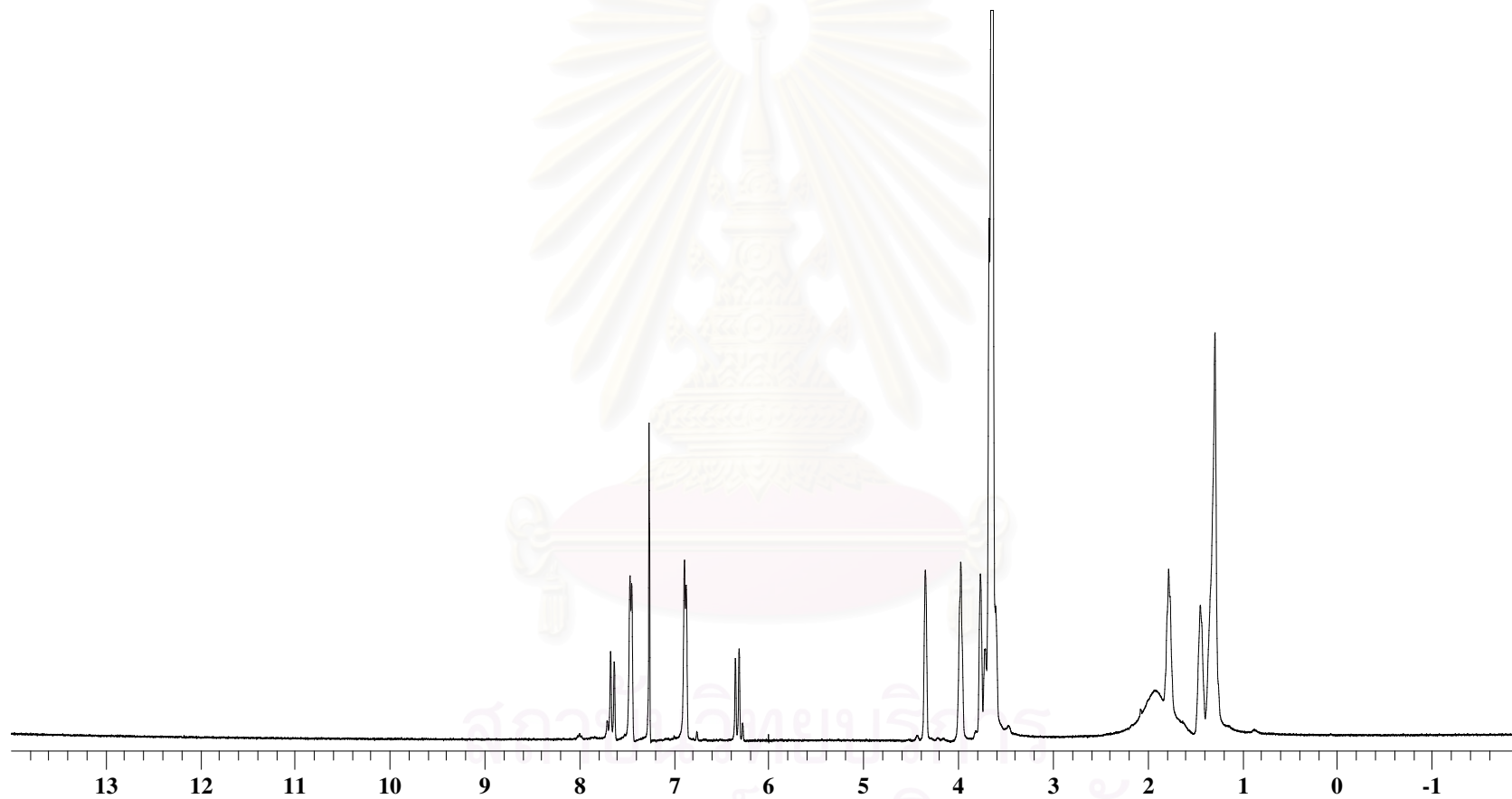
Figure B.18 Mass spectrum of poly((1,2-(bis(4-2-carboxyvinyl)phenoxy))ethane)-*co*-(poly(ethylene glycol)400)), **P2-PEG400**
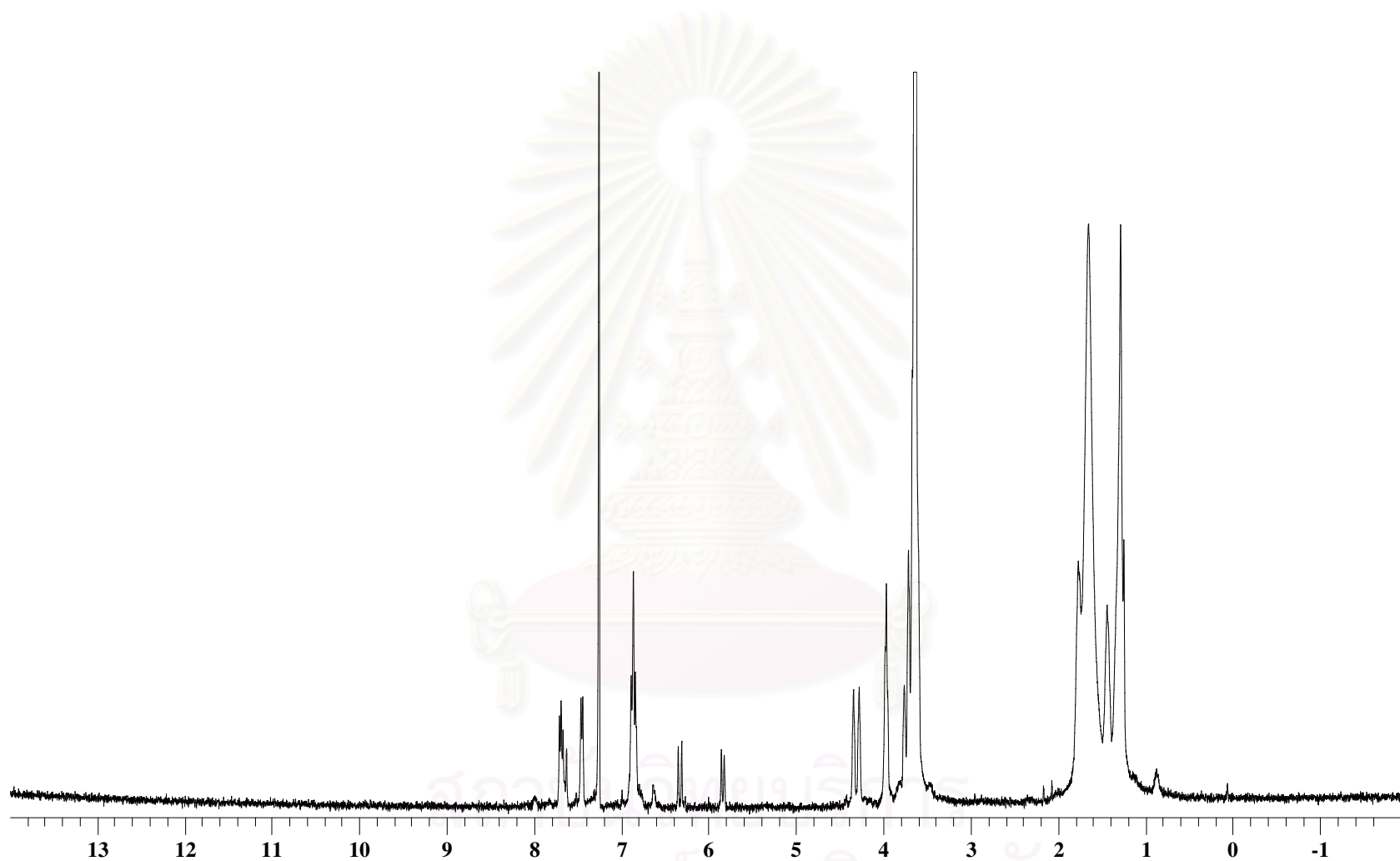
[MULDI-TOF MS]

Figure B.19 Mass spectrum of poly((1,2-(bis(4-2-carboxyvinyl)phenoxy))ethane)-*co*-(poly(ethylene glycol)400)), **P2-PEG400**
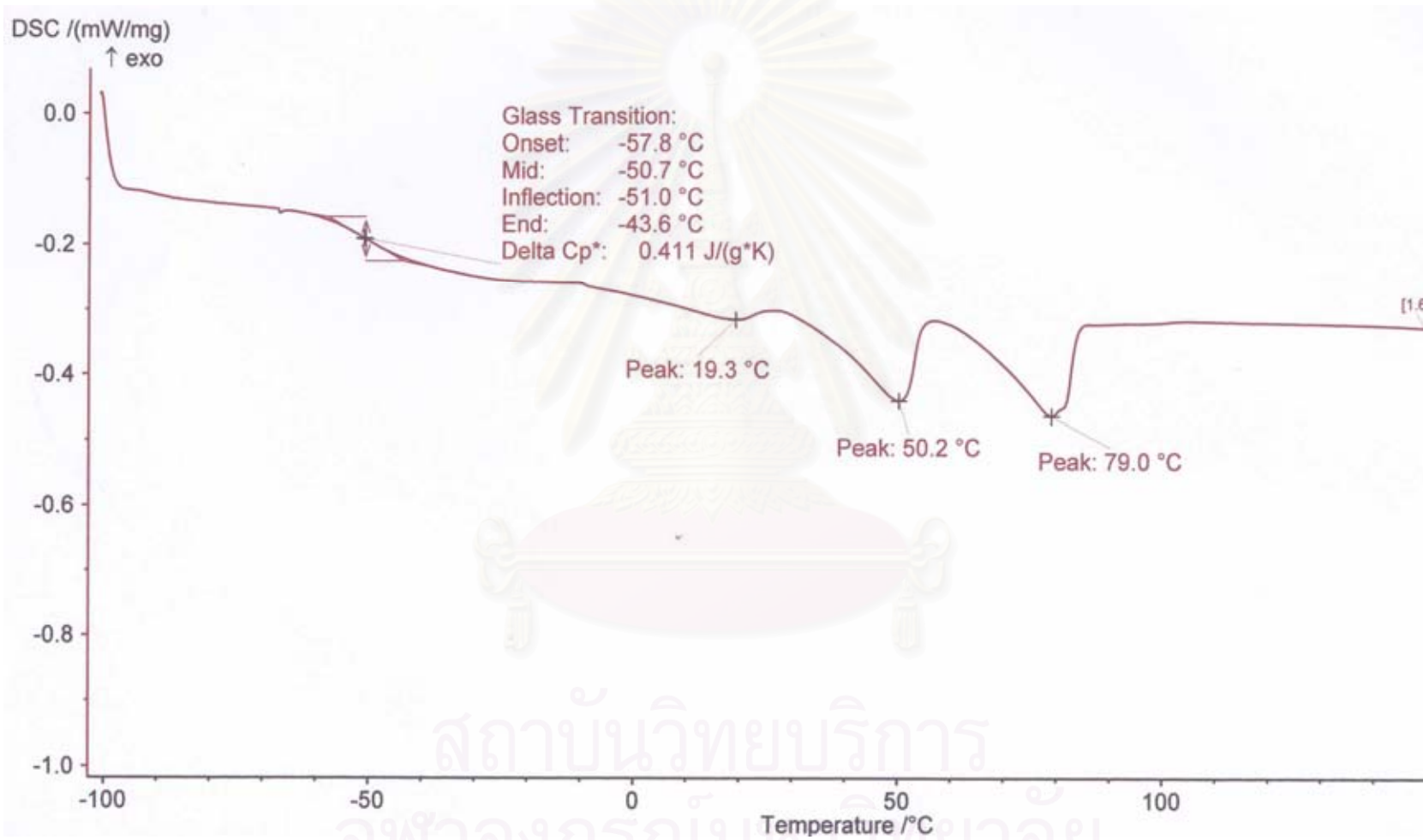
[ESI-MS]

Figure B.20 ^{1}H-NMR (CDCl$_3$) spectrum of poly((1,12-(bis(4-2-carboxyvinyl)phenoxy))dodecane)-*co*-(poly(ethylene glycol)400)),

P12-PEG400

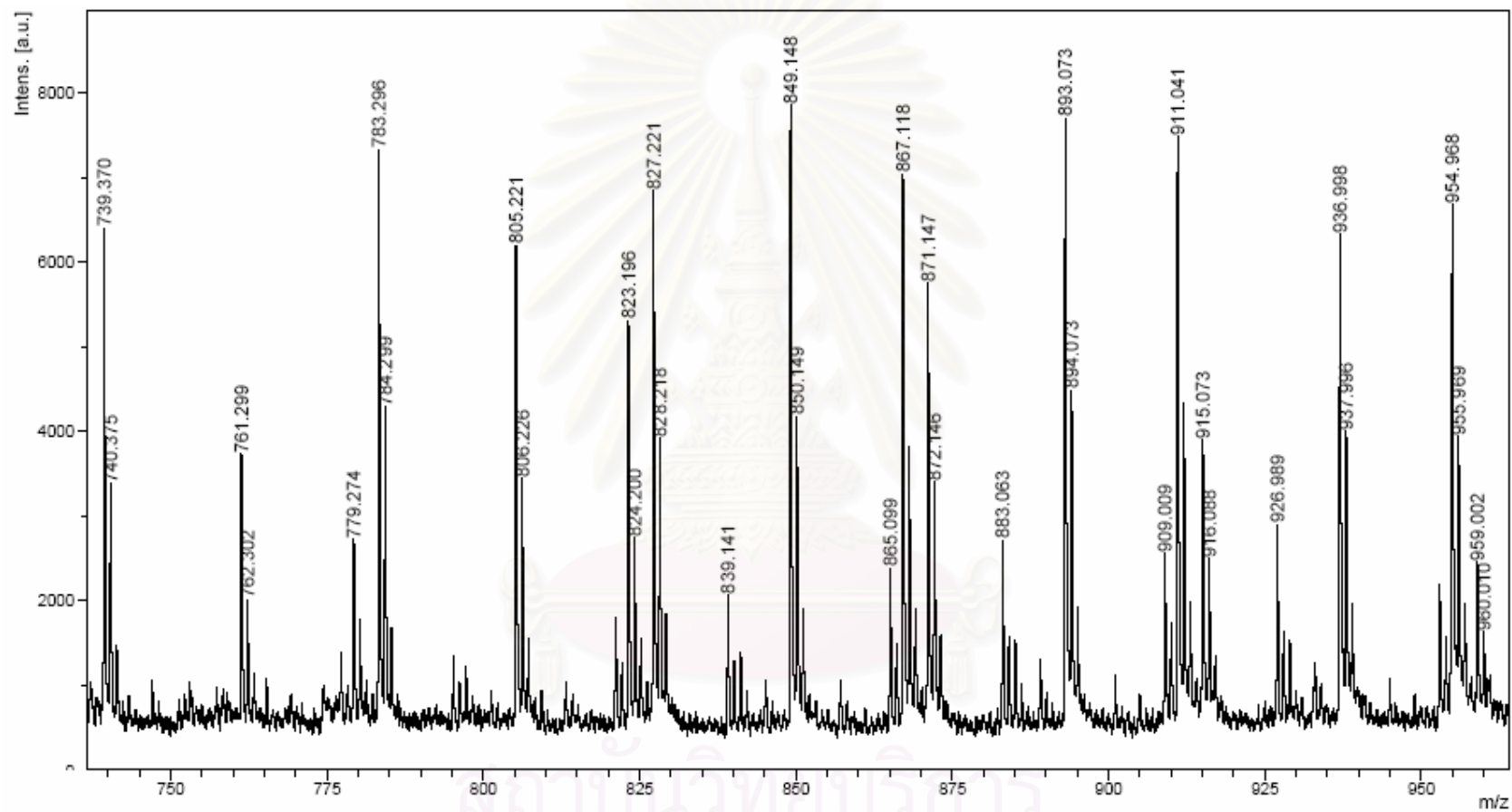**Figure B.21** ^{1}H-NMR (CDCl₃) spectrum of poly((1,12-(bis(4-2-carboxyvinyl)phenoxy))dodecane)-*co*-(poly(ethylene glycol)400)),

P12-PEG400 irradiated
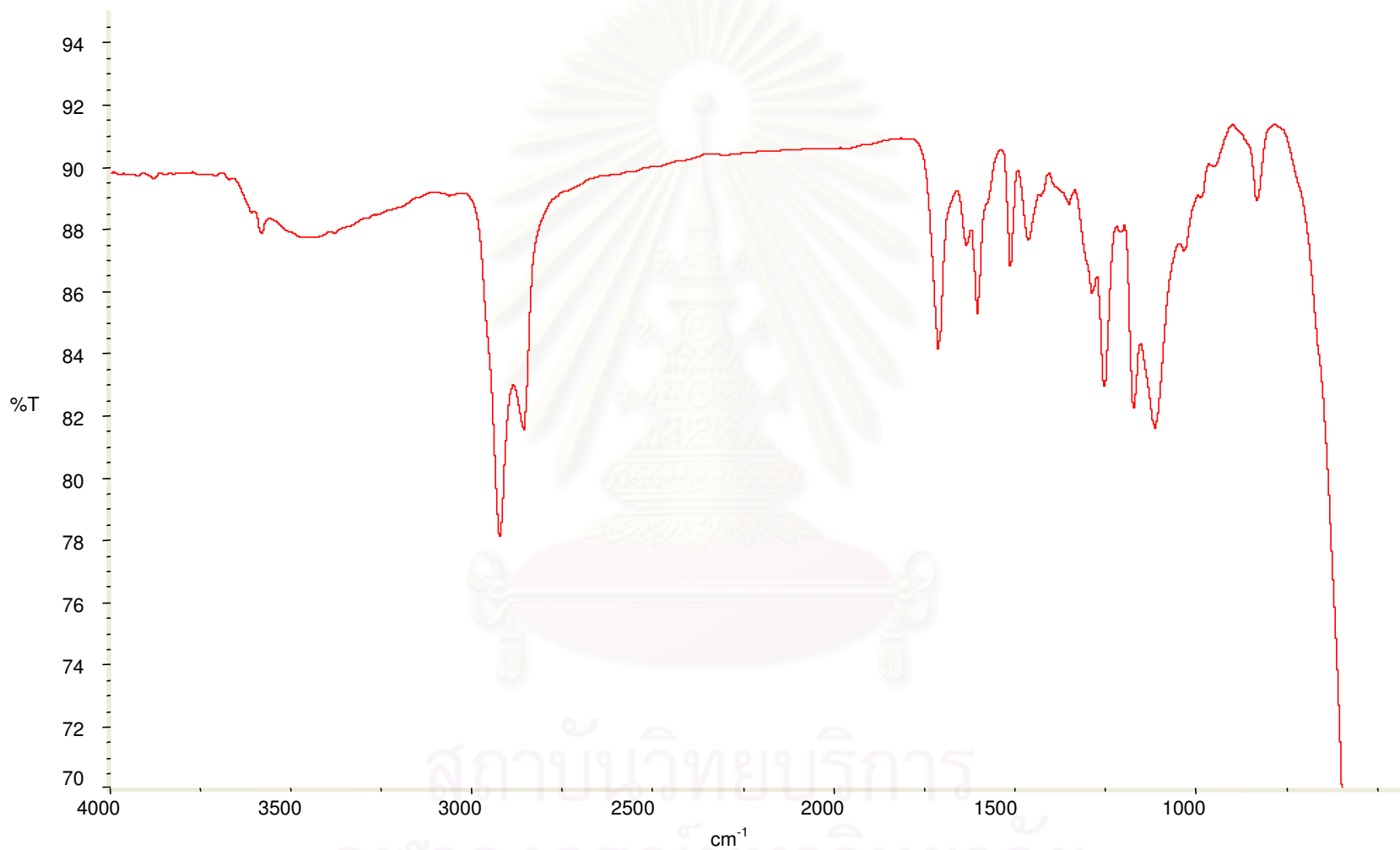
Figure B.22 FT-IR spectrum of poly((1,12-(bis(4-2-carboxyvinyl)phenoxy))dodecane)-*co*-(poly(ethylene glycol)400)), **P12-PEG400**

Figure B.23 DSC spectrum of poly((1,12-(bis(4-2-carboxyvinyl)phenoxy))dodecane)-*co*-(poly(ethylene glycol)400)), **P12-PEG400**

Figure B.24 Mass spectrum of poly((1,12-(bis(4-2-carboxyvinyl)phenoxy))dodecane)-*co*-(poly(ethylene glycol)400)), **P12-PEG400**

[MULDI-TOF MS]

VITA

Pruetinan Changhin born on May 14, 1982 in Lopburi, Thailand. She got a Bachelor's Degree of Science in Chemistry from Srinakharinwirot University in 2003. Then in 2004, she was admitted into Master Degree Program in Petrochemistry and Polymer Science at Chulalongkorn University. During her study towards the Master's Degree, she received financial support from Graduate School, Chulalongkorn University.

She address is 14/22, 14/23 Nikorn Village Piyaboot Road Banmee, Lopburi 15110.